Electrical Characterization of Electroporation of Human Stratum Corneum

by

Vanu G. Bose

BS Electrical Engineering, M.I.T., 1988
BS Mathematics, M.I.T., 1988

Submitted to the Department of Electrical Engineering and Computer Science
in partial fulfillment of the requirements for the degree of

Master of Science

at the

MASSACHUSETTS INSTITUTE OF TECHNOLOGY

February 1994

Author .....
Department of Electrical Engineering and Computer Science
January 25, 1994

Certified by .....
Dr. James C. Weaver
Senior Research Scientist
Harvard-MIT Division of Health Sciences and Technology
Thesis Supervisor

Accepted by .....
Frederic R. Morgenthaler
Chair, Departmental Committee on Graduate Students

Electrical Characterization of Electroporation of Human Stratum Corneum

by

Vanu G. Bose

Submitted to the Department of Electrical Engineering and Computer Science
on January 25, 1994, in partial fulfillment of the
requirements for the degree of
Master of Science

Abstract

Electroporation is a well established method for causing a tremendous enhancement of ionic and molecular transport across bilayer membranes, particularly cell membranes. Recently there has been interest in the electroporation of intact tissue for applications such as transdermal drug delivery and enhanced local chemotherapy. This thesis presents a study of the changes in the electrical impedance due to electroporation of human stratum corneum in vitro. There are two primary goals to the study: to test the hypothesis that electroporation occurs in the skin, and to relate these changes to previously observed changes in the transdermal flux of moderately sized (399 - 1,000 D) charged molecules. Electrical impedance measurements made before and after high voltage "pulses", applied to the human skin samples in vitro, were therefore investigated.

Thesis Supervisor: Dr. James C. Weaver
Title: Senior Research Scientist
Harvard-MIT Division of Health Sciences and Technology

Chapter 1

Introduction

Electroporation is a well established method for greatly enhancing ion and molecular transport across bilayer membranes, and is increasingly used to transport molecules across the membranes of single cells [1-4]. Recently, there has been interest in the electroporation of intact tissue, with potential applications such as transdermal drug delivery [5-7] and enhanced local chemotherapy [8-10].

Electroporation is a phenomenon appears to depend strongly on the time dependent transmembrane voltage, and which simultaneously results in both increased permeablization and local transport across lipid-bilayers driven by an electric field. Electroporation is achieved by the application of high voltage for a short period of time (typically 100 μs to 1 msec) across a bilayer membrane. Early studies of electroporation in artificial planar bilayer membranes demonstrated that very large and rapid electrical conductance changes accompany electroporation [11, 12].

This thesis presents a study of the changes in electrical impedance due to the application of one or a series of high voltage pulses to human stratum corneum (SC) in vitro. There were two primary goals of this study: to test the hypothesis that electroporation occurs in human skin, and to relate the changes in electrical impedance to the previously observed changes in the transdermal flux of moderate size, charged molecules under similar conditions [5].

It has been well established that the SC is the primary barrier to transdermal drug delivery [13, 14]. The SC is a layer of dead cells which comprise the top 10 - 20 μm of the epidermis (see fig. 1).

Within the SC there exist multi-lamellar, intercellular lipid bilayers. Cross sections of these layers can be seen in the electron micrographs of mouse skin, which is thought to be quite similar to human skin (fig. 2). It has been shown that the application of short duration high voltage pulses can significantly increase transdermal fluxes of model charged molecules [5]. Electroporation of these multilamellar layers within the SC is hypothesized to account for these increased fluxes.

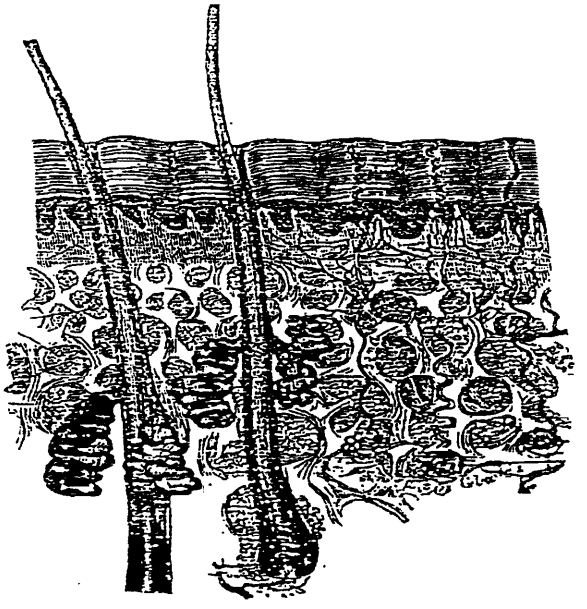

Figure 1: Cross section of human skin [15].

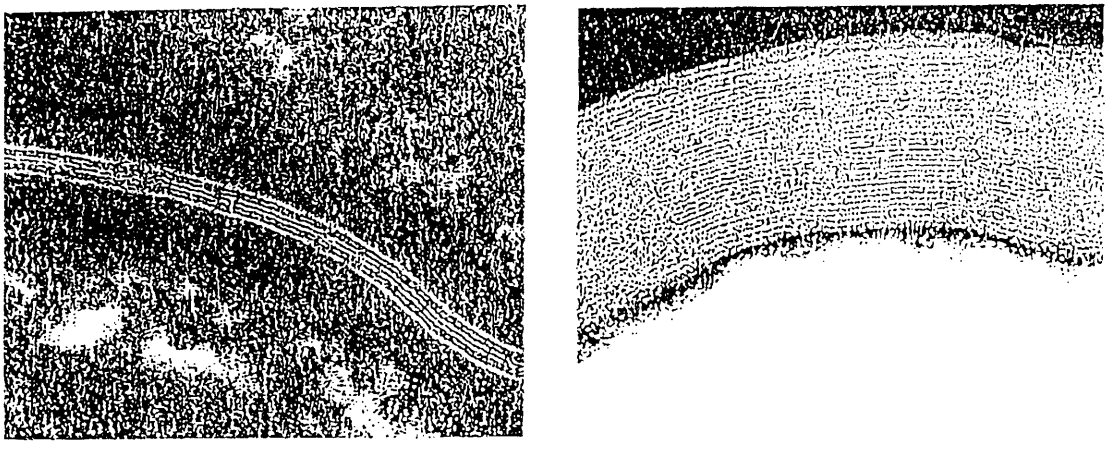

Figure 2: Electron micrograph of mouse skin [16].

In an electro-chemical system, such as electrodes immersed in physiological saline, electrical current is due to the movement of ions (e.g. sodium and chloride ions), mainly by electrophoretic transport, through the system. Thus, changes in electrical impedance will reflect the changes in the flux of these ions. Both sodium and chloride are relatively small ions with only a single charge each. However, changes in their flux may be correlated with the changes in flux of larger, more highly charged molecules, such as those used in a recent study. [7].

Chapter 2

Background

2.1 Electroporation

Electroporation is the simultaneous creation of a transient, high permeability state and electrically driven transport in bilayer membranes by the application of high voltage for a short (typically on the order of μsec) period of time. Electroporation has been observed and characterized for both natural and artificial planar bilayer membranes. Furthermore, electroporation theory predicts, and experimental observations have confirmed, that an electroporated planar membrane can experience one of four possible outcomes: 1) a slight increase in electrical conductance, 2) mechanical rupture, 3) incomplete reversible electrical breakdown (REB), or 4) reversible electrical breakdown [17]. Cell membranes are believed to exhibit similar, but not identical, behavior. The term "electrical breakdown" is accepted in the literature, but is misleading, as the "breakdown" actually refers to a conformational change in the membrane in response to the increased energy of the system resulting from the high voltage electrical pulse. The conformational change is believed to consist of perforating aqueous pathways ("pores"), and there are likely routes for the transport of both ions and molecules.

The high voltage pulse plays a dual role in electroporation: 1) it causes a change in the state of the membrane, and 2) can transport molecules through the membrane. The ability of electroporation to permeablize lipid bilayer membranes, and drive molecules across them, makes it a potential candidate for a transdermal drug delivery mechanism.

2.2 Transdermal Drug Delivery

Transdermal drug delivery offers many potential advantages over conventional routes of drug delivery [13, 14]. It allows drugs to enter systemic circulation, reducing degradation by the intestine, stomach or liver. This is especially important for new peptide drugs being developed, which are metabolized before entering systemic circulation [18]. Transdermal delivery could also allow for delivery over a long period of time, whereas conventional injections or oral delivery provide a high concentration of drug which then decays until the next delivery. For example, it would be desirable to have a controlled time profile release of insulin rather than three impulses of insulin each day. Additionally, transdermal delivery minimizes the issue of patient compliance, since a an external device could potentially contain enough drug for an entire treatment and deliver it appropriately. For example, patient compliance has become an alarmingly important issue in tuberculosis treatment. The tuberculosis symptoms disappear well before the course of treatment is finished, and many patients stop, or become less regular, with their medication. This incomplete treatment results in the incubation of the TB microorganism in the presence of anti-microbial drugs, which in turn selects for the resistant mutants. In short, such patients become walking incubators of resistant TB strains. As a result new resistant strains of tuberculosis can develop.

Some passive (partition plus diffusion) transdermal drug delivery systems are commercially available. Examples include nicotine delivery systems for people trying to quit smoking, estrogen replacement systems for the treatment of post-menopausal conditions, and nitroglycerin for the treatment of angina. This method is only useful for drugs which cross the skin fairly easily by diffusion. Many methods are currently being studied to enhance the flux of molecules that are not normally permeable to the skin. These include chemical enhancers, iontophoresis (the use of small current,

typically < 1 mA to drive charged molecules across the skin) and ultrasound [13, 14].

2.3 Skin Impedance

The study of the electrical properties of skin dates back to the initial discovery of the electrical properties of the skin by Vigouroux, in 1879 [19]. Since that time there have been many studies of the electrical properties of skin. Among the various effects studied were the connection between galvanic skin response and location on the body [20] , temperature and emotional stimuli [21]. Perhaps the most famous usage of skin impedance measurement is in polygraphs, where it is an important variable used to determine whether or not a person is telling the truth. It has been well established that the skin impedance varies greatly from subject to subject, and from location to location on a given subject [20]. Several different circuit models have been proposed for human skin. Ranging from the commonly used simple parallel RC circuit, to complicated non-linear models [22] intended to describe the low voltage non-linear behavior of the skin.

Clearly, the skin is not an electrically homogeneous material (see fig. 1). It has been well established that the SC has a much higher resistance than the underlying tissues [23]. The epidermis and dermis have high electrical conductivities, due to aqueous intercellular spaces and the network of blood vessels. The SC, having many lipid bilayers in series and very little water, has a significantly higher resistance.

The electrical properties of the SC are of particular interest to this investigation, since the SC is the primary barrier to transdermal drug delivery. The structure of the SC itself varies with depth. The junction between the viable epidermis and the SC is characterized by tightly packed keratinocytes and has been found to have a higher resistance than the outer, more loosely packed layers [23]. For this investigation it was necessary to first determine an appropriate

model to for the SC to provide a framework in which the changes due to the application of a short duration high voltage electrical pulse can be analyzed.

Chapter 3

Materials and Methods

The methods used were similar to those used by Prausnitz et al. [7] in their initial study of the transdermal flux of three charged molecules due to electroporation. The methods were followed as closely as possible so that changes in electrical properties could be compared with the established molecular flux results.

3.1 Skin Preparation

Skin samples were obtained from two different sources: 1) Cadaver skin was obtained within 48 hr's post mortem from autopsies performed at the Beth Israel Hospital (Boston, MA), and 2) frozen samples of surgical skin as well as additional cadaver skin samples were obtained from the National Disease Research Interchange (NDRI, Philadelphia, PA). Some samples obtained from NDRI were fresh and shipped overnight on ice, while others were flash frozen in liquid nitrogen and shipped on dry ice. Tissue was generally removed from the abdomen or back, just lateral to the midline, although tissue from the breast, and thigh have been used as well. Samples with little or no hair were used since the presence of hair often causes small tears during the heat stripping process. When samples with small tears are placed in the permeation chamber, the tears fills with saline, creating a very low resistance shunting pathway through the skin.

All of the samples were prepared using established preparation methods, full thickness samples were prepared by gently scraping off the subcutaneous fat. Epidermis samples were then heat separated by submerging full thickness skin in 60 ^{o}C water for 2

minutes and gently removing the epidermis [24]. All samples were stored at 4 ^{o}C / 95 % humidity for less than 2 weeks. This is a generally accepted procedure in the transdermal drug delivery research community.

The preparation of the skin samples required certain safety precautions. Most samples were screened for hepatitis and A.I.D.S., but precautions must still be taken since the tests are not perfect and there are other health risks (e.g. bacteria, for samples that are not frozen in liquid nitrogen). Surgical gowns, face masks, double gloving and eye protection were used when heat stripping the skin. After heat stripping, the samples were only used in a restricted area, and equipment was sterilized with Clorox after use.

3.2 Experimental Methods

Prepared skin samples were loaded into side-by-side permeation chambers , exposed to well-stirred phosphate buffered saline (PBS), and allowed to hydrate for 20 - 30 minutes. 37 ^{o}C water, controlled by an Endocal water bath (Neslab Instruments, Newington, NH), was run through the water jacket on the permeation chambers. Electric pulsing was applied with Ag/AgCl electrodes (In Vivo Metrics, Healdsburg, CA). An exponential-decay pulse (τ = 0.14 - 1.3 msec, GenePulser, Bio-Rad, Richmond, CA) was applied with the cathode on the SC side. The permeation chamber was placed in parallel with a 45 Ω, 5W resistor (see fig. 3). This resistor was much smaller than the resistance of the chamber plus electrodes (approx. 900 Ω) and ensured that the high voltage was delivered with a uniform time constant from sample to sample. A 5 Ω, 5W resistor was placed in series with the pulser output to protect the pulser in the event that the chamber was accidentally short circuited. The term "pulser voltage" denotes the voltage setting on the Bio-Rad pulser, "chamber voltage" denotes the voltage across the permeation chamber, and "transdermal voltage" denotes the voltage across the skin sample.

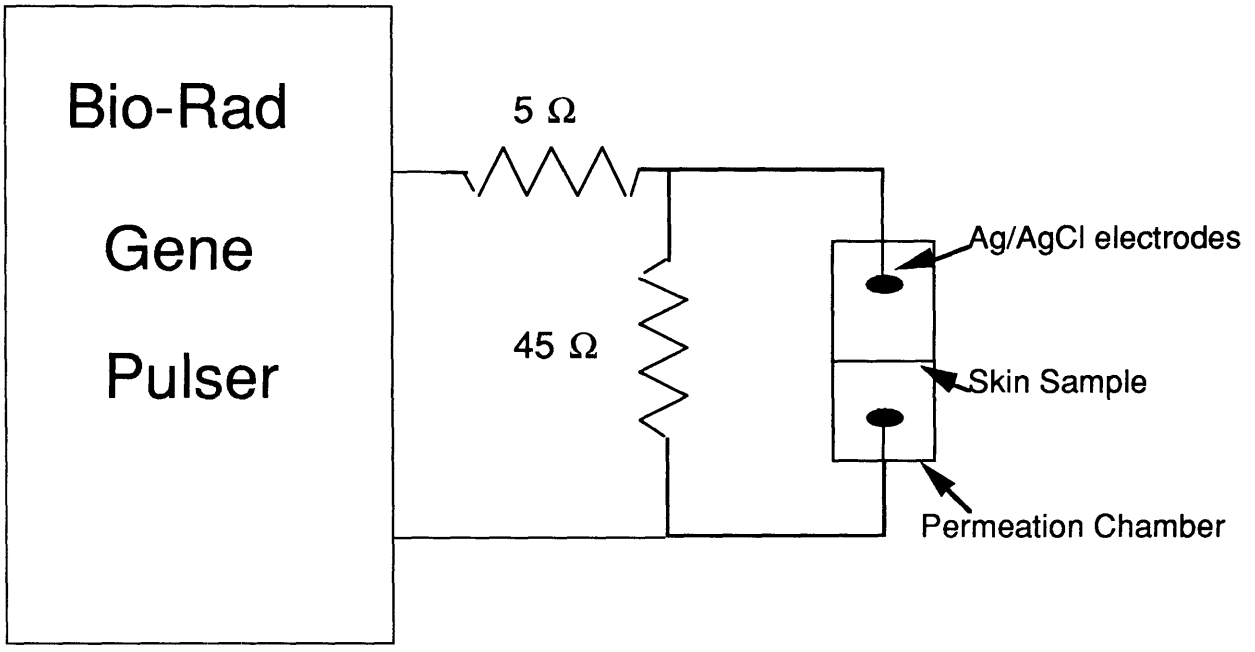

Figure 3: Experimental Setup

Reported voltages are transdermal values. During a pulse, the apparent resistance of the chamber, without skin (but including electrodes, saline, and interfacial resistances), was less than 1 kΩ. The electrodes have a non-linear current-voltage relationship at high voltages, which resulted in a significant voltage drop across the electrodes during high voltage pulsing. The non-linear nature of the electrodes was characterized empirically by measuring the current through and voltage across the chamber during a high voltage pulse. The current obtained by measuring the resulting voltage across a 5 Ω resistor placed in series with the chamber. The voltage was obtained by measuring the voltage across a second set of electrodes placed in the chamber with a high impedance differential amplifier. The high impedance input resulted in a very small current (order 1 μA) through the second set of electrodes, so the non-linear nature of this second set of electrodes was not important.

The apparent resistance of the chamber (R_{ch}) with skin varied from 900 ohms during lower-voltage pulses (~ 50 V across skin) to 600 ohms during higher-voltage pulses (~ 500 V across skin). Transdermal voltages were determined by calculating the ratio of the apparent skin resistance to the apparent total chamber (with skin) resistance. This ratio is equal to the ratio of the transdermal voltage to the voltage across the whole chamber (with skin). After applying a voltage pulse and measuring the resulting current, apparent resistances were calculated by dividing the applied voltage by the measured current. The relationship between the chamber voltage and the transdermal voltage was found to be best described by the following equation, which was found to hold for pulser voltages > 50 V.

$$V_{transdermal} = -6 \times 10^{-5} V_{chamber}^2 + 0.35 V_{chamber} + 5.4$$

3.3 Impedance Measurements

There are several constraints on the design of the impedance measurement system. The voltage developed across the skin during the measurement must be limited to a maximum of about 100 mV to insure that the tissue behaves in a linear manner [22]. Previous studies of skin impedance have shown a large range of values as different locations are used on the same subject, as well as from subject to subject. Furthermore, electroporation can cause a decrease in skin resistance of three orders of magnitude. Due to these variations the system must be capable of determining impedances that range from 10 kΩ to 1 MΩ. In vivo measurements present the additional constraints of electrical isolation and portability of the system. Specifically, the system must be electrically isolated to protect the subject, and the portability is important as the in vivo studies are usually done in animal facilities or in collaboration with other laboratories, and cannot be left in one location.

A four electrode system was chosen so that the impedance characteristics of the electrodes would not affect the measurements . A typical experimental setup, involved four electrodes for impedance measurement and two more electrodes for application of the high voltage pulses. A current ranging from 0.1 - 2 μA is passed through the outer electrodes and the resulting voltage across the inner electrodes, measured by a high input impedance (~1 GΩ) amplifier, is recorded. Another set of electrodes was used for high voltage application and impedance measurements, because the electrode properties change during the application of high voltage, and it takes a few seconds for them to stabilize after termination of a high voltage pulse.

In order to meet the electrical isolation and portability constraints, the system design was based on IBM compatible laptop computer (PCBrand 486 notebook, Moorpark,CA). Fig.4 shows a block diagram of the impedance measurement system. Communication between the computer and the measurement circuitry was done through a bi-directional parallel port. Data was alternately written to the D/A converter (which provides the measuring wave form) and read from the A/D converter (which is a digital representation of the voltage across the inner electrodes). The sampling rate was controlled by the software, which established the read/write rate to the converters. The data read from the A/D converter is then stored on disk for later analysis. A detailed description of the system can be found in Appendix A.

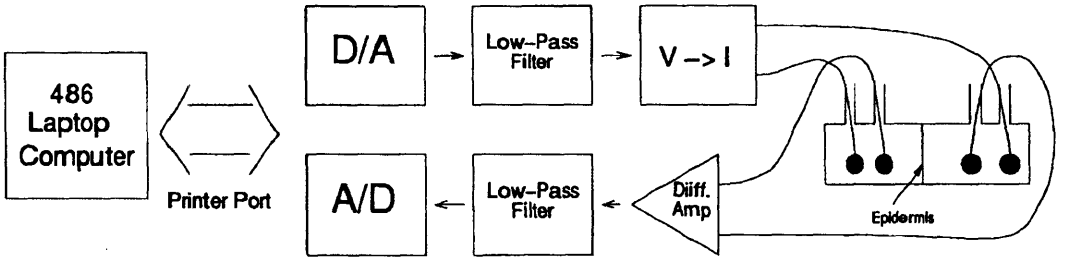

Figure 4: Block Diagram of Impedance Measurement System. Communication between the computer and the measurement circuitry was done through a bi-directional parallel port. Data was alternately written to the D/A converter and read from the A/D converter, at a software determined rate. The output wave form was converted to a current and applied across the outer two electrodes. The voltage across the inner electrodes was measured by a high input impedance (~1 GΩ) amplifier, low pass filtered to prevent aliasing and then digitized and stored in the computer.

The background noise in the system was significant. a large component of the noise was due to 60 Hz power line interference, which was significantly reduced by placing a ground plane under the experimental chamber and twisting the wires leading to it. However a background level on the order of 10 mV peak-to-peak over the measured frequency range remained.

For impedance measurement, several different wave forms were considered, including steps, chirps and pseudo-random noise. A 100 msec duration step was chosen as the standard measuring excitation for two reasons: a high signal to noise ratio and insensitivy to the 8-bit quantization of the output wave form. Furthermore, producing a step excitation is fairly simple, making the method readily applicable to any in vivo device where monitoring electrical impedance is important. Commonly reported values for a simple parallel R-C circuit model of the skin are on the order of 100 kΩ for resistance and 10 nF for the capacitance [20]. A circuit with

these values has a cutoff frequency of 1 kHz. A 10 kHz sampling frequency was chosen as it should be sufficient to capture the significant features of the skin impedance. This required that the lowpass filters have a cutoff frequency just below 5 kHz. During initial experiments the impedance was monitored for several hours after pulsing. From these data it was determined that monitoring for 20 minutes after pulsing was sufficient to determine the degree of recovery of the SC (i.e. the resistance did not change significantly between 20 minutes and 2 hours after pulsing).

Because the dominant characteristics of the skin are primarily at low frequencies (i.e. less than 1 kHz), the step response must be measured for times significantly longer than 10 msec to be accurately characterized. Since the frequency response rolls off at about 10 dB/decade from 10 Hz to 1 kHz, the signal-to-noise ratio at 1 kHz is approximately 20 dB worse than at 10 Hz, for a noise power level constant in frequency (the background noise level in the experimental chambers was of order 10 mV). If the step response is taken for times shorter than 10 msec, the low frequency behavior must be extrapolated from the result. This extrapolation from a high signal-to-noise ration to a low one is very sensitive to noise. However, as will be shown, changes in the impedance immediately after electroporation can occur on a much faster time scale (on the order of 100 msec) than can be accurately measured. These rapid changes occurred at times less than one second, and by one second post-pulse the changes in the impedance had a time constant on the order of one second. However, it is possible to obtain qualitative information for times less than one second after the pulse.

Starting at 20 msec post-pulse, a repeated wave form was applied that consisted of a two msec current square wave followed by four msec of zero current. Since the resistance of the sample is increasing during this time, the voltage developed across the skin during the two millisecond application of current will take longer than two milliseconds to decay. It was empirically determined that a four millisecond waiting period was more than sufficient for the

voltage to decay. The two millisecond square wave was therefor used to obtain the impedance of the sample, but as discussed before this measurement is not very accurate due to the noise present in the system. It is for this reason that the measurement at one second post-pulse (the first 100 msec measurement) is used to compare impedances measured before and after the pulse, and measurements made before one second are discussed only qualitatively.

3.4 Computer Control

The 486 laptop computer was used to coordinate the experiments and data acquisition. The Bio-Rad Gene Pulser was modified (see Appendix A) so that the computer could trigger the pulser. When the pulser was triggered, relays were used to connect the pulser output to the chamber, and to isolated the impedance measurement system from the high voltage. An end of pulse (EOP) signal was obtained from the pulser and was used to trigger the start of the impedance measurements. The software for controlling the experiments was written in Turbo C++ (Borland, Scotts Valley, CA). Examples of present versions of the software are included in Appendix B.

The current during the pulse was monitored by placing a 5 ohm resistor in series with the chamber. The voltage across this resistor was monitored by an oscilloscope (Hewlett Packard HP54602A) which was interfaced to the 486 laptop through a serial port interface. The data from the oscilloscope were downloaded into the computer after all of the impedance measurements were completed.

The other serial port on the computer was connected to the serial port on a Sun Sparc2 workstation (Sun Microsystems, Mountain View, CA). This link was used to transfer data to the workstation for analysis.

3.5 Data Analysis

The recorded step response was stored on disk for later analysis the workstation using the Matlab software package (MathWorks Inc., Natick, MA). The first goal of the data analysis was to determine an appropriate model for the SC. The frequency domain data was fit to several different complex impedance polynomials. The model must have at least one more pole than zero since existing data [20] shows that the impedance function rolls off as frequency increases. Polynomials with more than two poles were found to have too many degrees of freedom, as they provided several different solutions for the same data. These constraints left only two candidate impedance functions: a model with one zero and two poles and a model with only a single pole (the latter corresponds to the traditional parallel R-C model of the skin). The pole zero representation for the two models are:

$$H(s) = K \frac{1}{(s + p)}$$

for the simple parallel RC circuit, and

$$H(s) = K \frac{(s + z)}{(s+ p1)\,(s+p2)}$$

for the model with one pole and two zeros. Where s is the complex frequency ($j\omega$).

Table 1 shows a comparison between these two models. The ratio of the mean square errors averaged over twenty different samples is presented in the table. The higher order model is an

improvement if the ratio is small. If this ratio is close to one, then the higher order model is not an improvement over the parallel R-C model. The ratio should never be greater than one, as the higher order model has more degrees of freedom and should always yield a slightly better fit to experimental data. It is clear that before pulsing the higher order model is a much better representation of the skin. However after pulsing it is only an improvement if the pulsing voltage was below approximately 400 volts transdermal. It will be shown that the transdermal resistance decreases after pulsing, with the magnitude of the change being greater for higher voltages. For very high pulsing voltages the transdermal resistance is so low that it effectively shunts the other of elements in the skin, using a simpler model is appropriate under these conditions.

	Before Pulsing	After Pulsing (< 400 V)	After Pulsing (> 400 V)
Ratio of Mean Squared Errors	0.11	0.14	0.99

Table 1: Average of the mean square error of the fits to a parallel RC model divided by average mean square error of the fits to the proposed model. If the value is much smaller than one, the proposed model is a significant improvement over the traditional R-C. Before pulsing, the proposed model is clearly superior, however after pulsing it is only significant for lower pulsing voltages (< 400 volts, transdermally). The averages were taken over twenty different samples.

The parameters of the frequency domain model are the poles, zeros and gain factor of the complex impedance function. To obtain the frequency domain data, the response was first differentiated to obtain the impulse response. The Fourier transform of the impulse

response was then fitted to obtain the frequency characteristics of the system. Some typical impedance measurements of human skin (without electroporation) and their corresponding fitted curves are shown in fig. 5. As reported in the literature, there is a wide range of skin impedance values. However, each of these curves has the same dependence upon frequency .

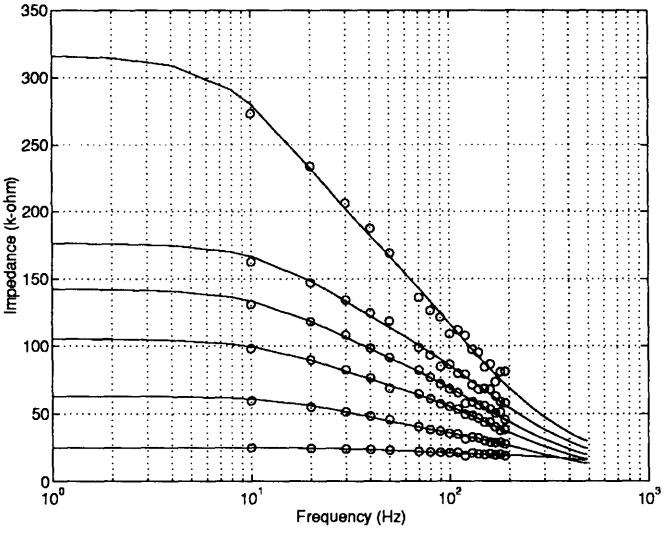

Figure 5: Typical measurements (magnitude of impedance) of human skin (without electroporation) with curves fitted to impedance model. Each curve is from a different piece of skin, to demonstrate variability in skin impedance. All curve have the same dependence upon frequency, the apparent differences for the lower curves are just due to the scaling of the graph.

Unfortunately, a pole-zero representation of a system does not yield a unique circuit model. Additional information, here knowledge of the structure of the skin, was used in determining the topology of the equivalent circuit. The circuit model shown in fig. 6 is one possible representation of the pole-zero fit and is viewed as the best because it is an extension of the parallel R-C circuit model most commonly used in the literature. R1 is the transdermal resistance. That is, R1 is a lumped model of the DC conduction pathways through the skin (e.g. sweatducts and hair follicles prior to pulsing). The remaining elements (C1 as well as the series

combination of R2 and C2) are proposed as a lumped representation of other conduction pathways and capacitance within the skin. Examples of such pathways would be through bilayer membranes and the intervening spaces, or through the corneocytes and their surrounding lipid regions. R2, C1 and C2 are intended to represent a lumped combination of all pathways except those that are purely ohmic in nature. For the remainder of this thesis, all resistance and capacitance values mentioned will be for a 1 cm^2 sample.

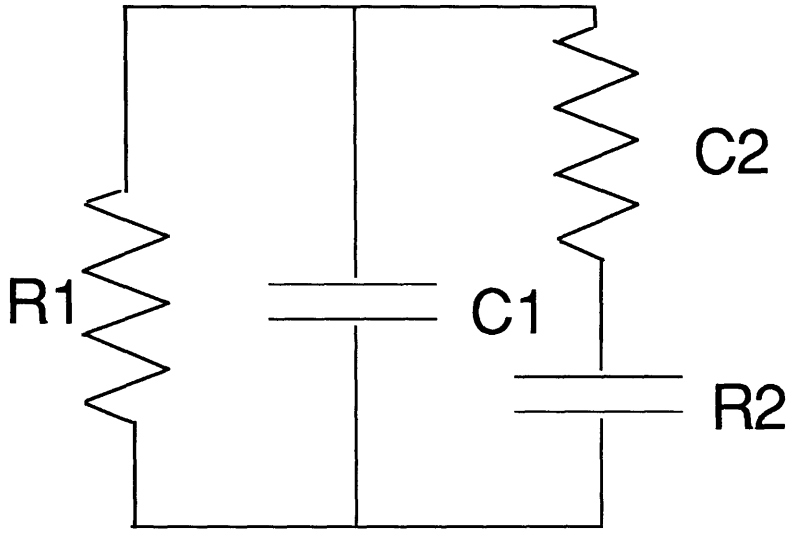

Figure 6: Lumped parameter model for skin used here. For a 1 cm^2 sample, typical element values are: 10 kΩ - 1 MΩ for R1, 100 kΩ – 1 MΩ for R2 and 10 -50 nF for both C1 and C2. All values mentioned here, and for the remaineder of this thesis, are for a 1 cm^2 skin sample.

Chapter 4

Results

As discussed previously, the impedance of skin varies greatly from donor to donor and even from location to location on the same donor. Therefore it is not surprising that the maximum change, recovery rate and degree of recovery the circuit element values after electroporation were also found to vary significantly from sample to sample. For this reason each study was performed with samples from the same general location on one donor. The general character (i.e. similar changes were found, but occurred at different voltages for different sample sets) of the changes was found to be similar across sample sets, but the magnitudes of the changes differed significantly.

4.1 Single Pulse Experiments

Fig. 7 shows typical impedance measurements before and for several times after pulsing. The curves drawn through the data for each measurement are those corresponding to the previously described fitted model. The top trace is the impedance before pulsing, and the bottom trace is the impedance at one second after pulsing. After pulsing, the impedance slowly returns toward its initial value. This recovery can be either complete (i.e. the impedance returns to within one percent of its pre-pulsing value) or incomplete depending upon the pulsing voltage and the particular sample.

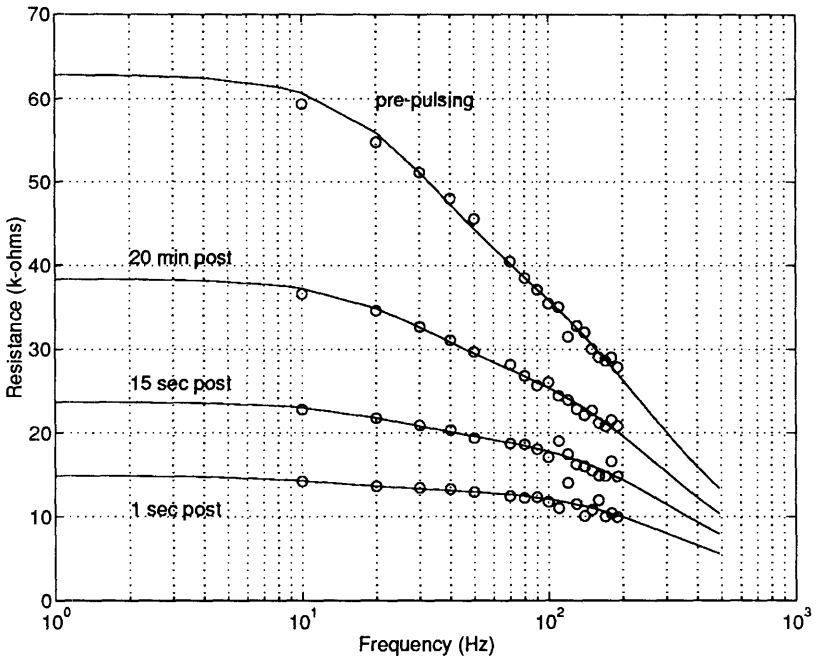

Figure 7: Typical measurements before and for several times after pulsing (magnitude of impedance shown v.s. frequency)

Fig. 8 shows the calculated values for the circuit elements between 1 second and 20 minutes after a pulse of 210 volts. The most significant change occurs in R1, the transdermal resistance. In fact, as the pulsing voltage increases, R1 decreases to a level where it effectively "short circuits" the other elements in the model, making determination of the other elements very inaccurate because of noise. This was verified by the mean square-error test presented in the previous section. As a result it was not possible to reliably determine the recovery dynamics of R2,C1 and C2., and the discussion of C1 and C2 is limited to the magnitude of the observed changes and not the dynamics of the change. R2 is not discussed quantitatively at all, and the only consistent qualitative feature is that its value decreases as a result of pulsing, and then recovers to a varying degree over time. In partial summary, the measurements of R2, C1 and C2 for high pulsing voltages, where R1 can decrease up to 3 orders of magnitude, are very sensitive to noise and are therefore not discussed quantitatively. An illustration of measurements of R2,

C1 and C2 are presented in figure 8. The sets of data shown in fig. 8 are not typical, but are instead one of the better sets of measurements of R2,C1 and C2, and were obtained from a experiment at a lower pulsing voltage.

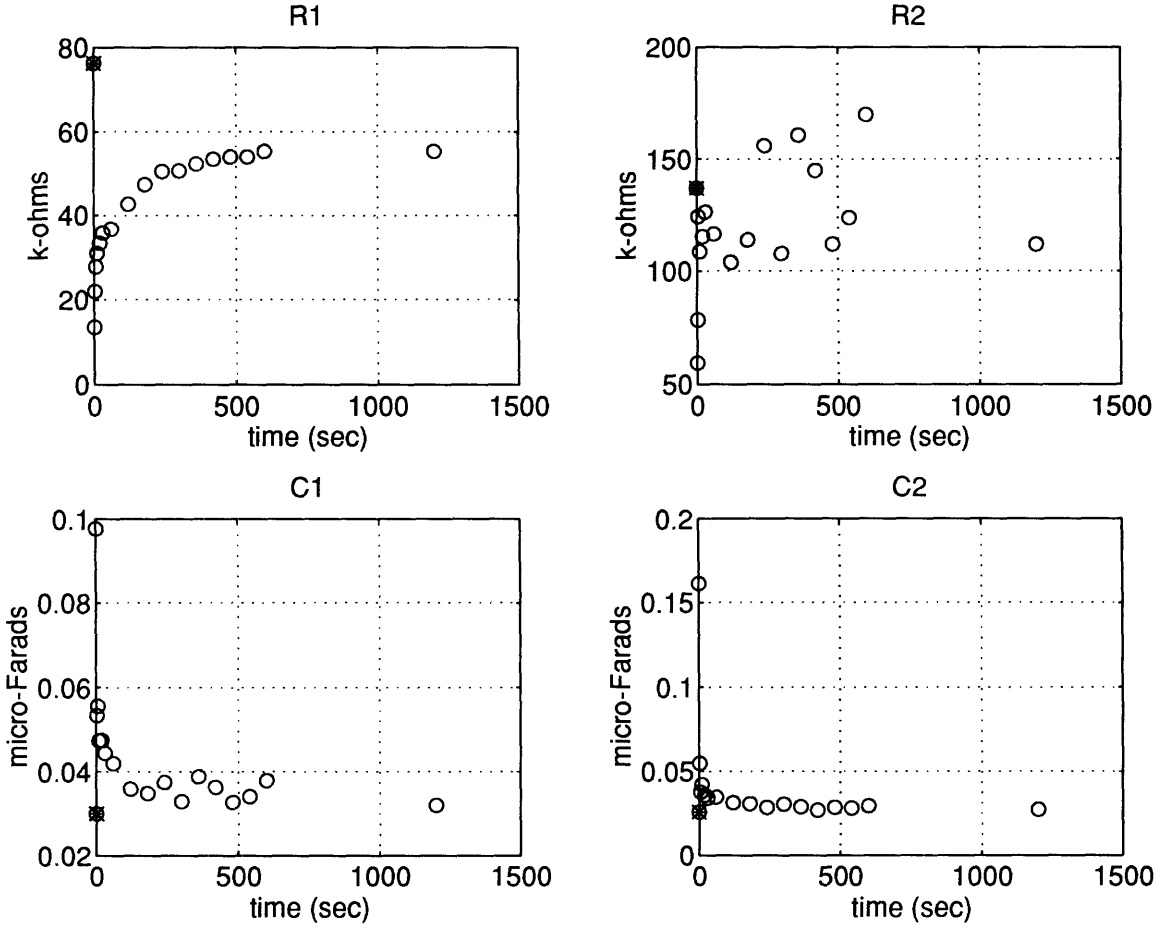

Figure 8: Circuit element values between 1 second and 20 minutes post-pulsing.

It is important to note that for low voltages (the actual voltage value depends upon the particular sample), where small changes in conductance are first observed, the process is reversible. Here "reversible" means that the conductance returned to within 1% of it's pre-pulsing value. If a second pulse, identical to the first is applied after the resistance has recovered, the resulting resistance change is

the same (within experimental noise limits) as it was for the first pulse. The existence of a voltage region over which the changes are reversible is consistent with theoretical and experimental results of the electroporation of lipid bilayers [1-4]..

4.2 Changes in Transdermal Resistance

The change in the transdermal resistance (R1 of fig. 6) is the most significant change in the model due to high voltage pulsing and interpreted as electroporation. The resistance as a function of time after the pulse typically has three distinguishable time constants on the order of 100 msec, 1 sec, and 100 sec ($\tau 1$, $\tau 2$ and $\tau 3$ respectively). It is important to note that the impedance measurements began 20 msec after the pulse, and there is some evidence for the existence of a recovery time constant of order less than 10 msec, since the apparent resistance at the onset of the pulse (presented later in this thesis) is much lower than the resistance measured before or 20 msec after the pulse. However, a characterization of the changes less than 20 msec after the pulse was not part of this thesis.

For reasons outlined earlier, it was not possible to obtain accurate resistance values for short duration measurements. For this reason it was not possible to quantitatively analyze the rapid changes occurring at times less than one second after pulsing, however we can qualitatively asses the characteristics during this time period. Fig. 9 shows the voltage developed across the chamber due to a 1.4 μA 2 msec current step applied every 6 msec, beginning at 100 msec after pulsing. Typically the recovery time constant is on the order of a few hundred msec and is consistent within a given sample set. In some cases, this time constant is not present (i.e. no changes on the order of 100 msec are evident) if the skin sample is too old. (i.e. stored at 4 ^{o}C and 95% humidity for more than ten days between heat stripping the skin and performing the experiment).

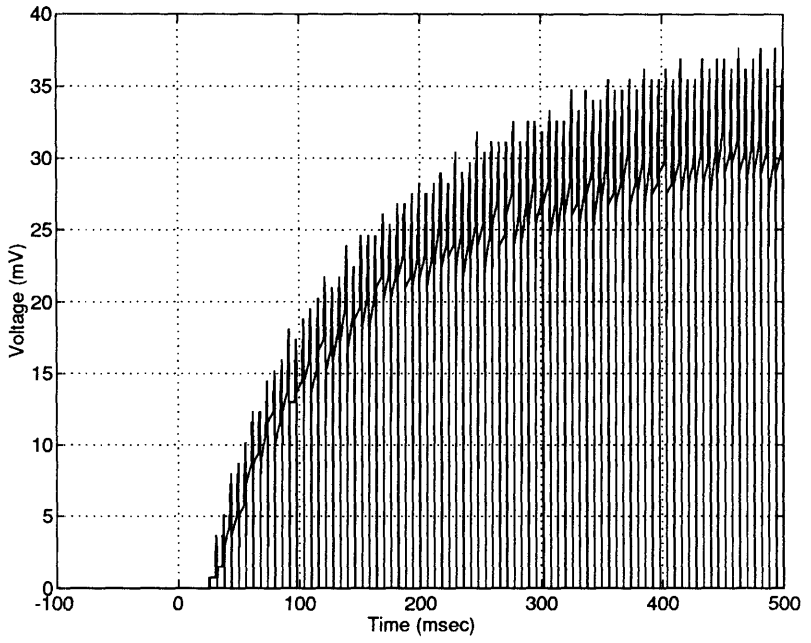

Figure 9: Transdermal voltage resulting from a series of 1.4 μA, 2 msec current step applied every 6 msec, between 100 and 540 msec post pulsing.

Panel A of fig. 10 shows R1 between 1 sec and 20 min. fit to two exponential functions for a typical sample. Panels B and C of the same figure show the fit a single exponential to the data over regions where the particular time constant is dominant. Since the recovery times constants are so widely separated, a single exponential is sufficient to describe the recovery process over each limited time range.

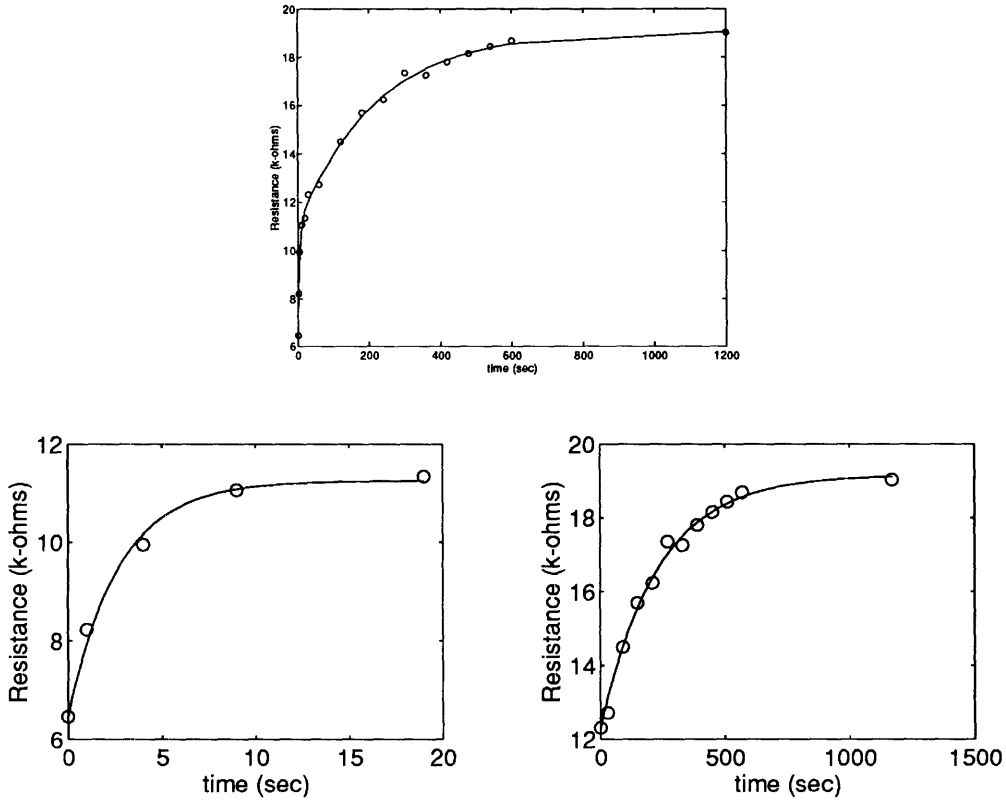

Figure 10: R1 between 1 second and 20 minutes after a typical pulse

Fig. 11 shows the transdermal conductance (normalized to the pre-pulsing conductance) at one second after pulsing for several different voltages. The data shown were collected from samples from a small area on the same donor (male cadaver, skin removed from a 7" x 3" area on the back). Each data point represents the average of 2-3 experiments. Each experiment was performed on a different skin sample: only one pulse was applied to each sample. This data (as well as data from other samples) show three distinct regions: A low voltage region where only a small increase in conductance occurs, a region slightly higher in voltage where the magnitude of the change increases with voltage and a region still higher in voltage where the magnitude of the change seems to have saturated.

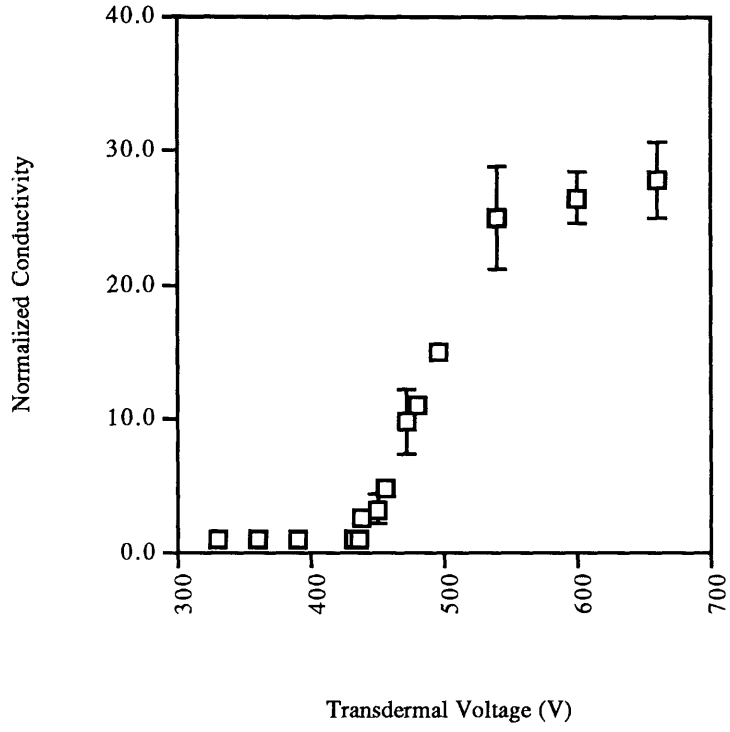

Figure 11: Normalized conductivity one second after the application of a 0.14 msec exponential pulse. Conductances are normalized to their pre-pulsing value.

The electroporation threshold, taken to be the voltage at which the transition to the steepest sloped region occurs, is consistent within a given sample set, as is the general dependence of the conductivity changes upon voltage. However this threshold varies from donor to donor, as well as with other factors which will be discussed later. It is important to note that the conductance after pulsing for even the highest voltages is still significantly smaller than the conductance of the chamber without skin (i.e. chamber filled with only saline, found to be approximately 900 Ω).

Another important aspect of the conductance changes is the recovery process., in particular the rate and degree to which the conductance recovers after electroporation. Fig.12 shows the conductance at twenty minutes post-pulsing for the same set of

samples shown in fig.11. Three regions are present , just as found in the data for change in the conductance after one second.

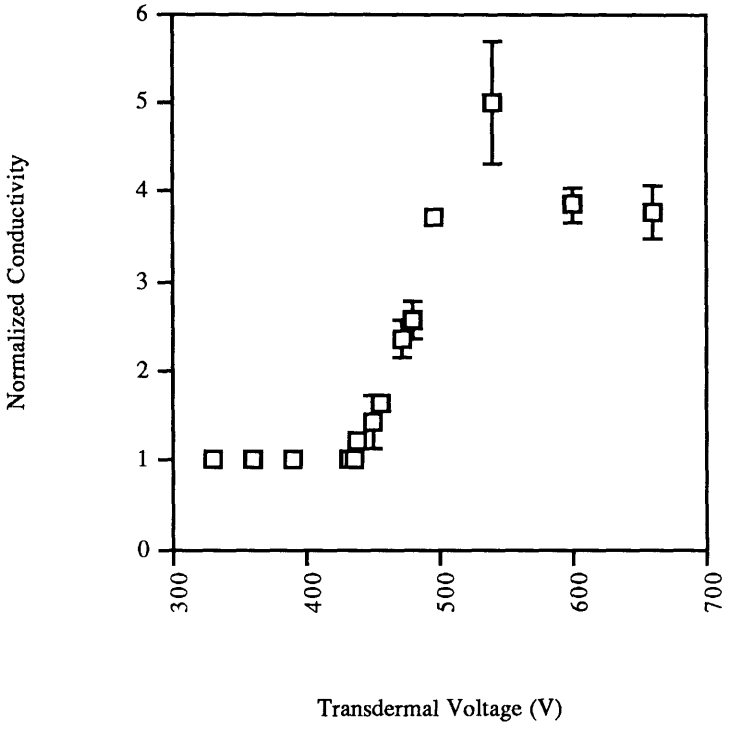

Figure 12: Normalized conductivity 20 minutes after the application of a 0.14 msec exponential pulse. Conductances are normalized to their pre-pulsing value.

For higher voltages, incomplete recovery implies that some permanent changes have been made to the skin, and this could be interpreted as damage to the skin. To asses the degree of damage done to the skin, the worst case recovery of electroporation was compared to a more conventional, purely mechanical means of drug delivery: a 28g needle. The needle stick was done on a full thickness skin sample, because the stripped skin samples were too delicate and would tear when punctured with a needle. It is well established [23] that the electrical resistance of the skin is primarily due to the SC, so a comparison of the changes in resistance between full thickness and stripped skin should be valid. Fig. 13 shows the change in impedance of the full thickness sample due to a 28g (o.d. 0.036 cm) needle stick. The resistance after the needle stick was approximately 6 kΩ, which is comparable to the post-pulsing

resistance observed after very high voltage pulses (e.g. 650 volts across the skin). However, for pulsed skin, the resistance recovers after pulsing but the resistance change due to a needle stick does not recover. After recovery from the application of a single high voltage pulse, the resistance was never lower than that observed after a needle stick, and was comparable to the resistance after a needle stick only for the highest voltage pulses used (e.g. > 450 V). Since the resistance is a measure of the conductive pathways through the skin, it is reasonable to assume that electroporation compromises the barrier function of the skin to a lesser degree than an injection with a 28g or larger needle.

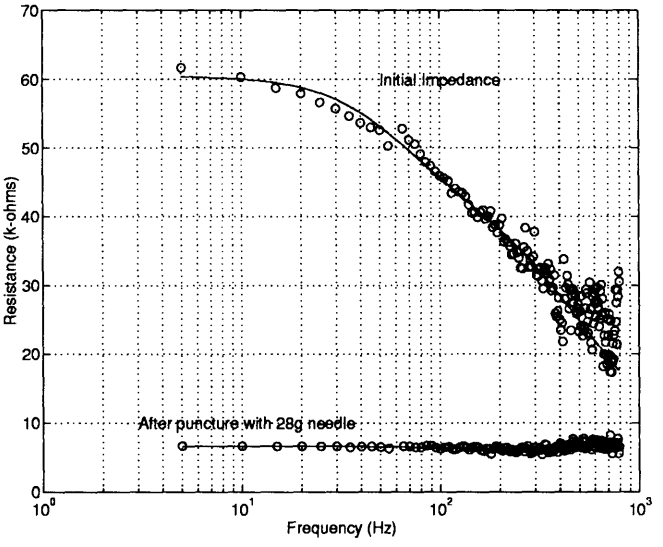

Figure 13: Change in the magnitude of the impedance due to a 28g needle stick

Figures 14 and 15 show the dependence of $\tau 1$ and $\tau 2$ upon pulsing voltage, for the same samples shown in the conductance graph. There is significant variation of these time constants, even within a given sample set, as evidenced by the large error bars. The general trend for the longer time constant is an increase with increasing pulsing voltage. Given the variability in the shorter time

constant it is difficult to draw any conclusions about its dependence upon pulsing voltage.

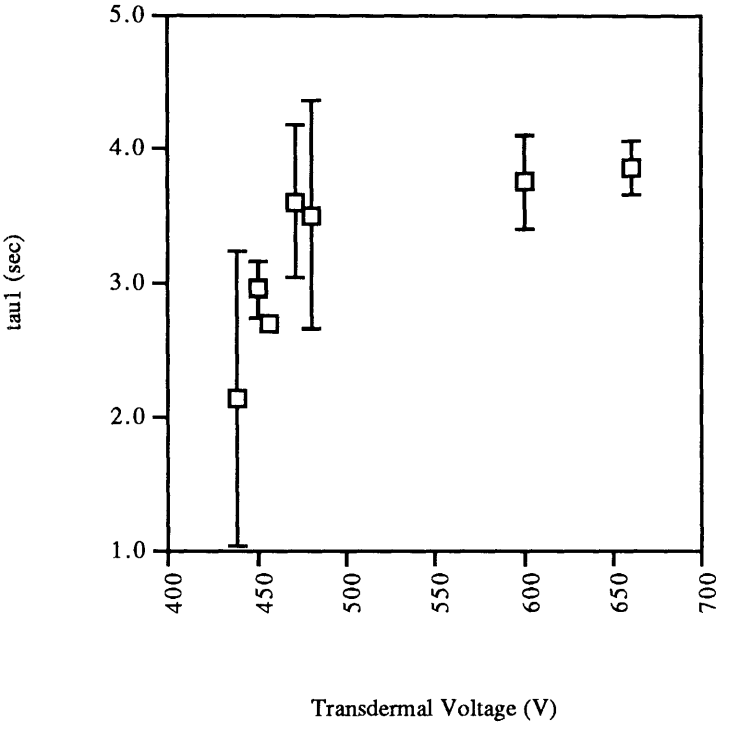

Figure 14: τ2 v.s. pulsing voltage, for a 0.14 msec exponential pulse.

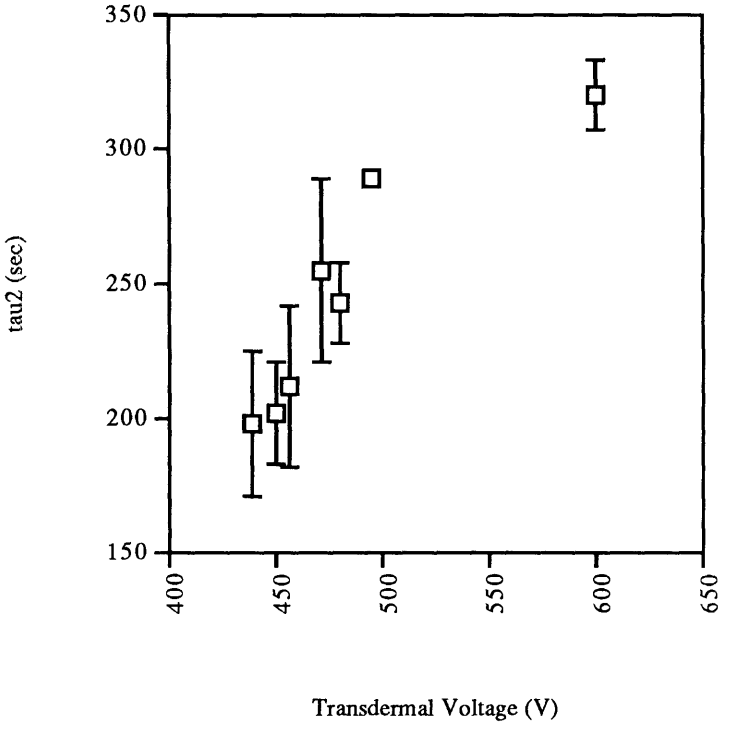

Figure 15: $\tau 2$ v.s. pulsing voltage, for a 0.14 msec exponential pulse.

4.3 Effect of High Voltage Pulse Time Constant

The effects of two different types of exponential pulses were investigated. The time constants were varied by changing the internal capacitor of the Bio-Rad Gene Pulser while keeping the external resistance constant. Capacitances of 25 μF and 3 μF were used, resulting in time constants of 1.3 msec and 0.14 msec. The experiments were performed using samples from the same area of the same donor (again cadaver back skin). The only difference from the previous study was that a sample was re-used if the resistance returned to its pre-pulsing value. This was justified because the results for a given high voltage pulse are completely reproducible if the sample exhibits full recovery. Figures 16 and 17 show the change in conductance at one second and 20 minutes after pulsing, each data point represents one sample. Resistance, instead of conductance, is plotted here so that the behavior at low voltages can be seen more clearly. The resistance has been normalized to the pre-pulsing value. As discussed previously, the resistance reaches steady-state within 20 minutes.

As observed before, there are three different types behavior exhibited by the resistance after pulsing. For example, the data for the two pulsing time constants are clearly different. To cause the same decrease in resistance, a higher peak voltage is required for the 0.14 msec high voltage pulse. However, these two sets of data differ only by a scaling factor in voltage. Fig.18 shows the two sets of data, normalized to be one at their threshold values. The difference in scaling factors is 0.48 (i.e. $V_{(1.3\ msec)} = 0.48 * V_{(0.14\ msec)}$). Here the value plotted is resistance instead of conductance, so that the overlap at low voltages is evident. The threshold was found to occur when the resistance one second after pulsing is about 80 % of it's pre-pulsing value. The general behavior of the resistance after pulsing as a function of voltage is the same, but the magnitude of this change as

a function of voltage varies with the pulsing time constant. The slope of the three regions are nearly identical, and their threshold values are very close.

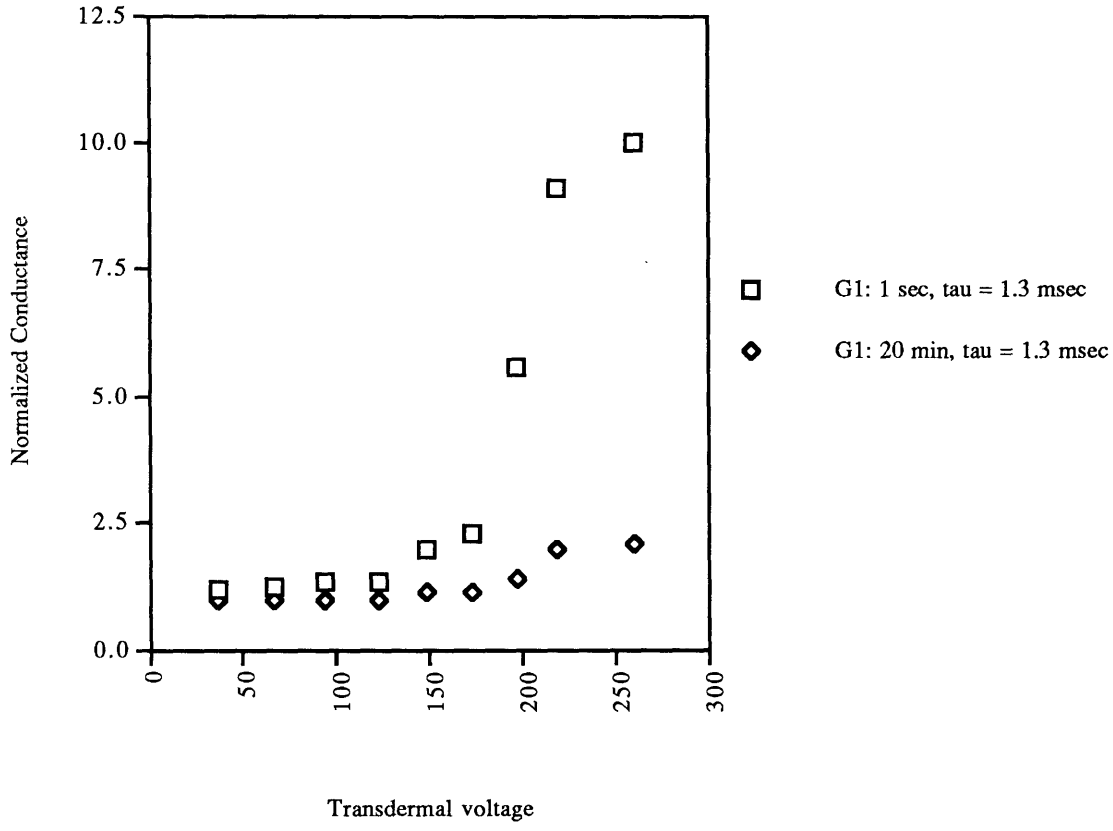

Figure 16: Normalized conductance at 1 second and 20 minutes after pulsing with an exponential pulse with time constant 1.3 msec. Conductances are normalized to their pre-pulsing value.

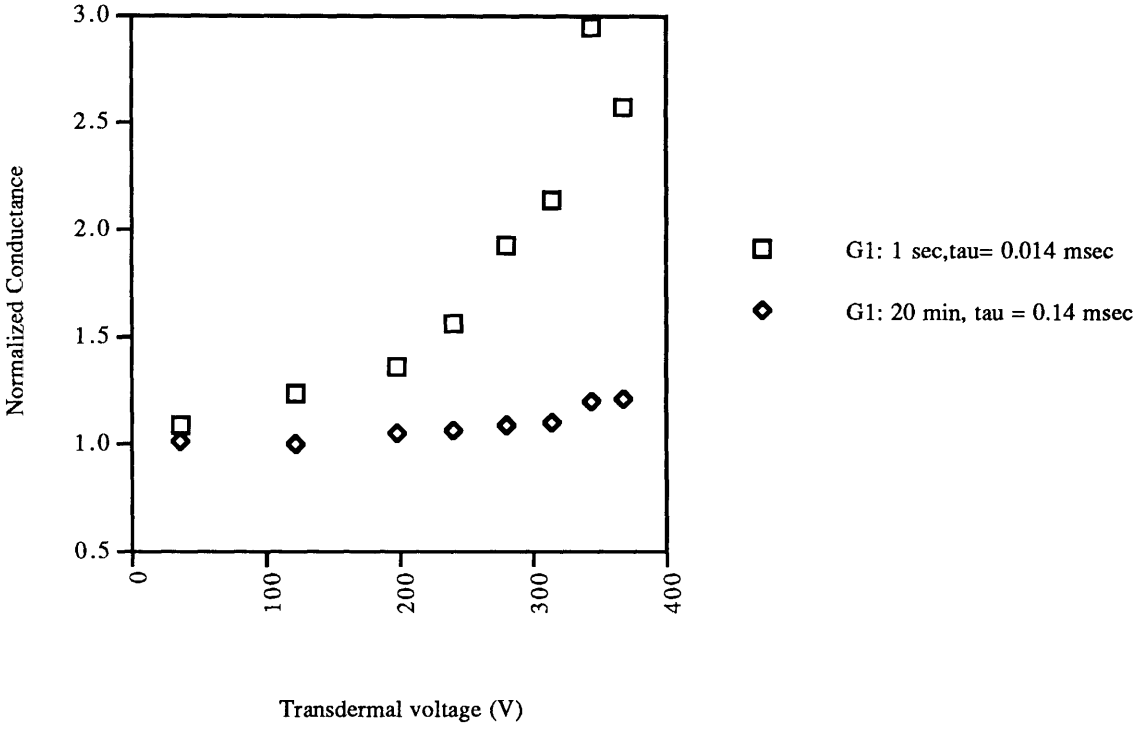

Figure 17: Normalized conductance at 1 second and 20 minutes after pulsing with an exponential pulse with time constant 0.14 msec. Conductances are normalized to their pre-pulsing value.

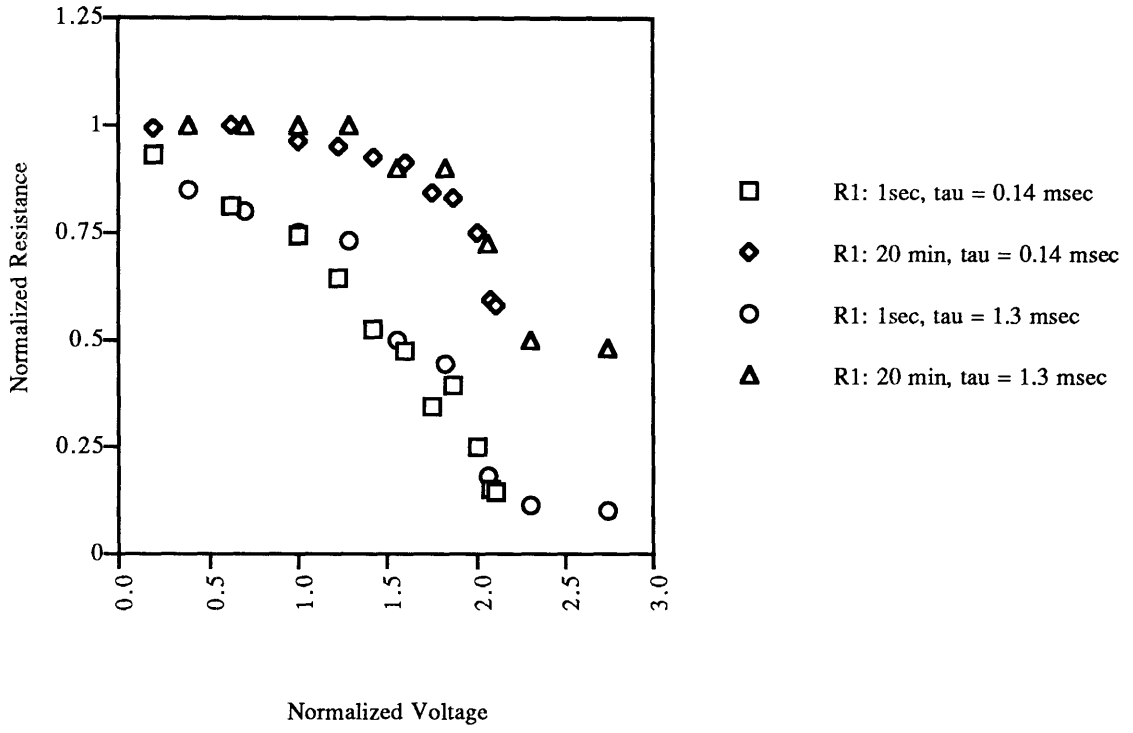

Figure 18: Resistance changes due to exponential pulses with time constants of 1.3 msec and 0.14 msec. Measured at 1 sec and 20 min. after a single pulse. Voltages are normalized to be one at their threshold values (the value at the onset of the region of steepest slope).

Fig.19 shows the difference between the resistance at 20 minutes and 1 second after pulsing, with the same voltage normalization used in fig. 18. This is a measure of the portion of the resistance change that is not reversible. This difference appears to increase linearly until the voltage at which the change in resistance at 1 second saturates. For voltages below this saturation more conductive pathways through the skin are created as the voltage increases, but a greater percent of this additional change can be completely reversed. Once saturation is reached the difference decreases. This seems to suggest that the changes induced in the skin when maximal change in resistance has been reached are different from the corresponding changes at lower voltages. As expected from

the data in figure 18, the data from the two different time constants agree well.

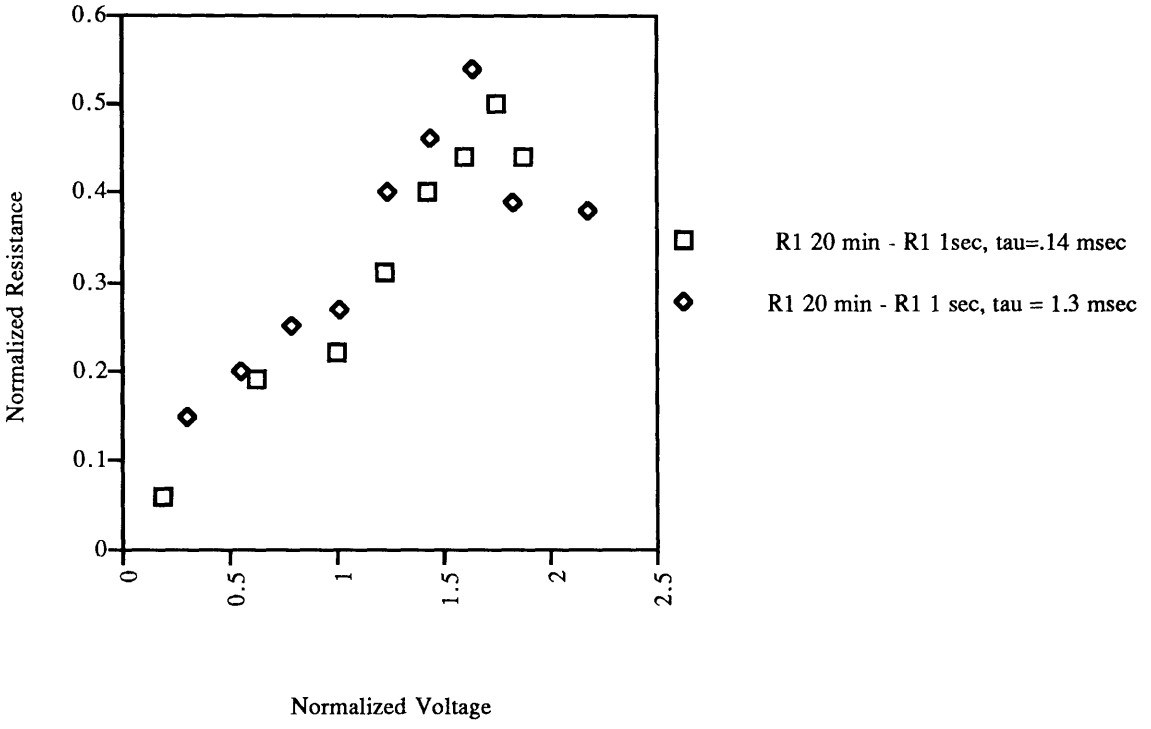

Figure 19: Difference between resistance (R1) at 20 min. and at 1 sec, for pulsing with two different exponential time constants. Resistances are normalized to their pre-pulsing values and voltages are normalized as in fig. 18.

4.4 Changes in Capacitance

The nature of the changes in capacitance are quite different from those of the resistance. Figures 20 and 21 show the change in the two capacitance values for the experiments performed with the 1.3 msec time constant. The three distinct regions are not evident, instead the capacitance appears to vary smoothly with voltage. The capacitance values for high pulsing voltages are not calculated for reasons discussed earlier. For most samples examined, the capacitance at one second after pulsing increased quadratically with voltage. However, the voltage dependence is only consistent within a given sample set. The capacitance value at twenty minutes post

pulsing either returned to the pre-pulsing value or, for higher pulsing voltages, to a slightly higher value. Although this increase is slight, and the results were quite noisy, there was a slight increasing trend observed in all of the experiments.

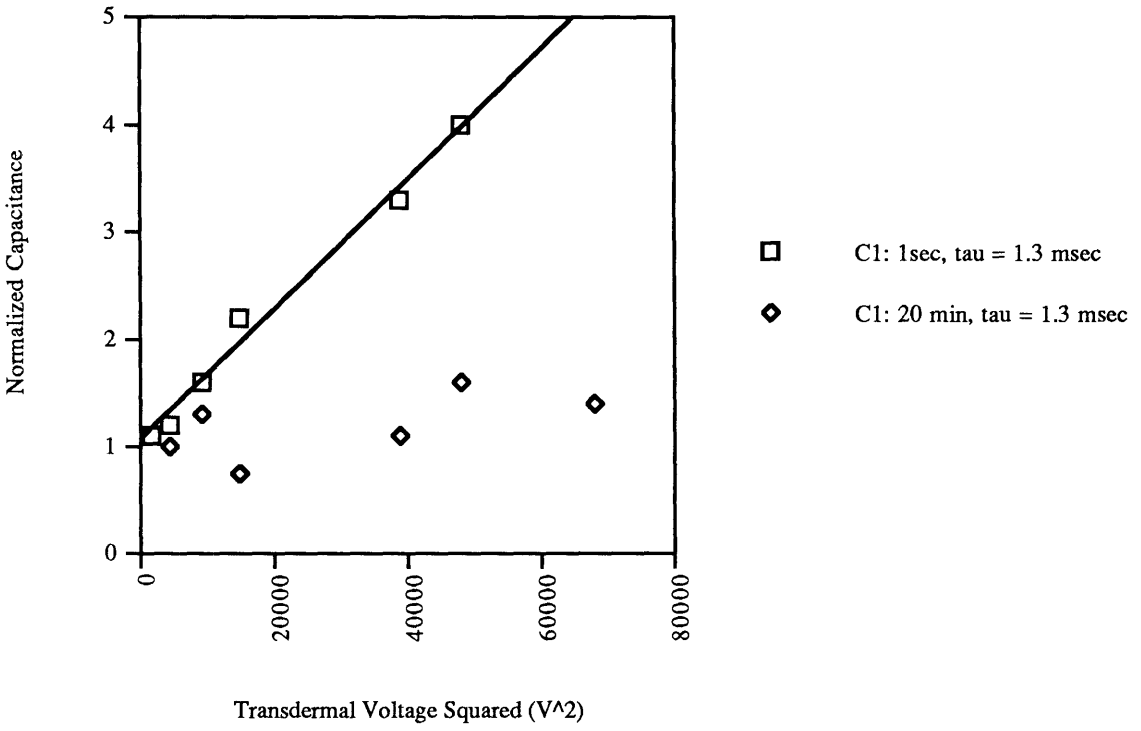

Figure 20: Change in C1 for a 1.3 msec exponential pulse. Capacitance values are normalized to their pre-pulsing value.

The comparison between the change in capacitance for the 0.14 and 1.3 msec time constants shown in figures 22 and 23 illustrates another difference between the behavior of the capacitance and the resistance after pulsing. The data are again normalized to the threshold value, but here the curves do not overlap as they did for the transdermal resistance.

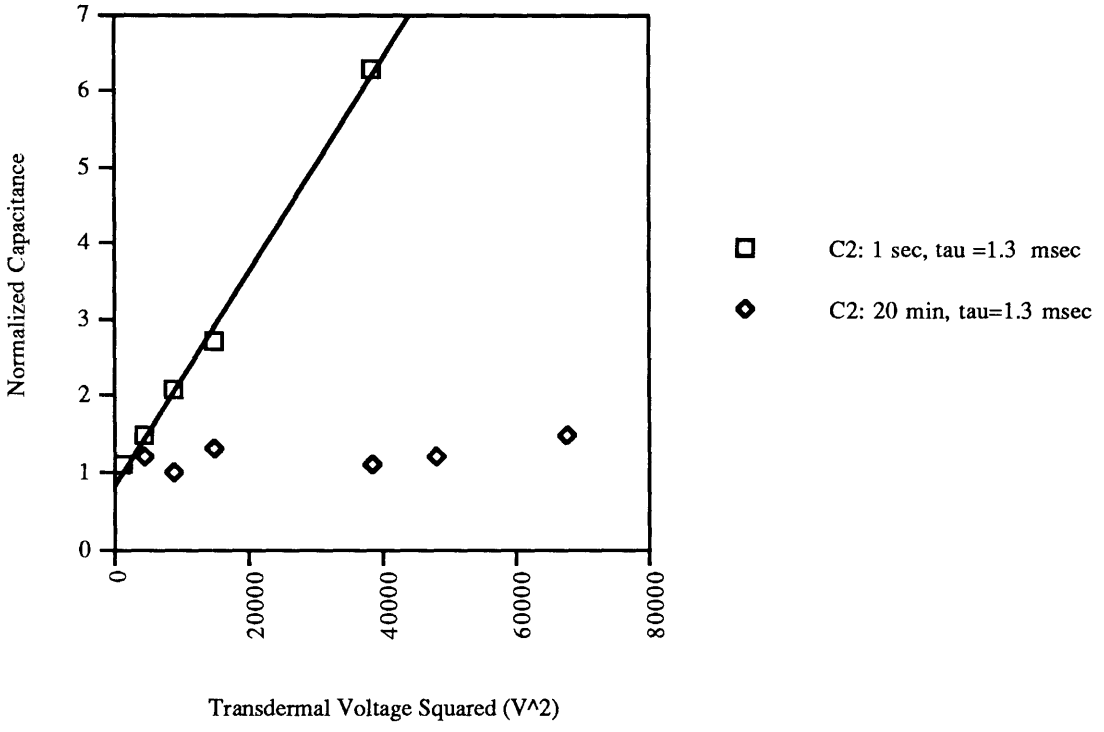

Figure 21: Change in C2 for a 1.3 msec exponential pulse. Capacitance values are normalized to their pre-pulsing value.

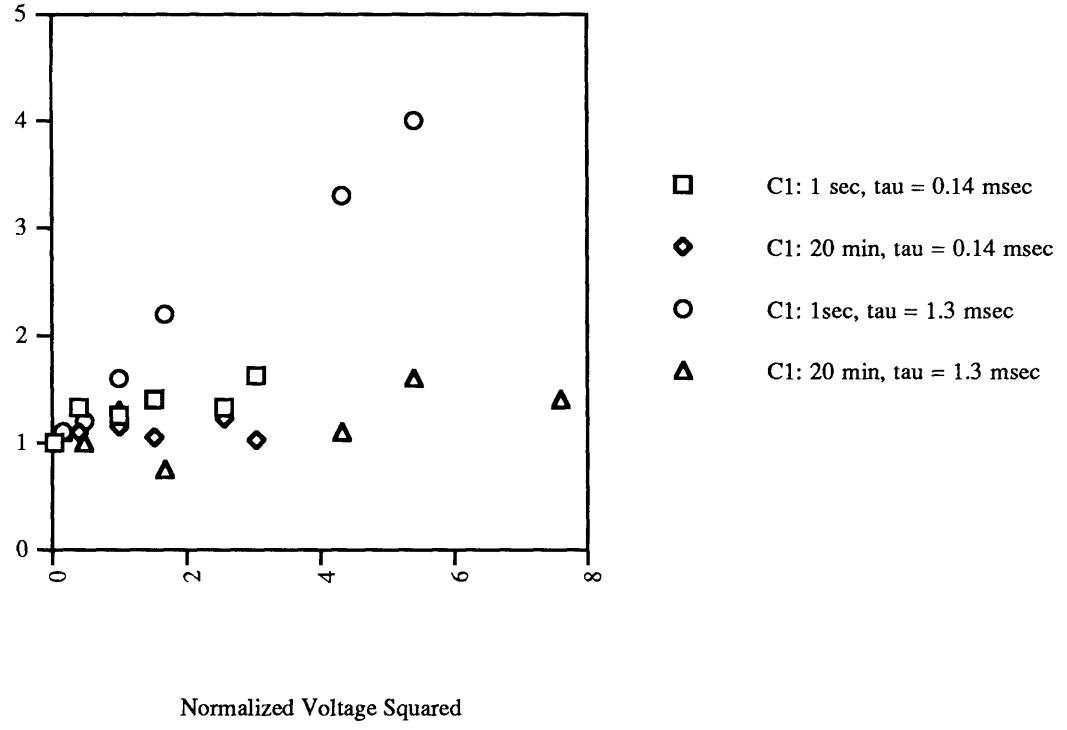

Figure 22: Comparison of the change in C1 for 1.3 msec and 0.14 msec time constants. Capacitance values are normalized to their pre-pulsing value.

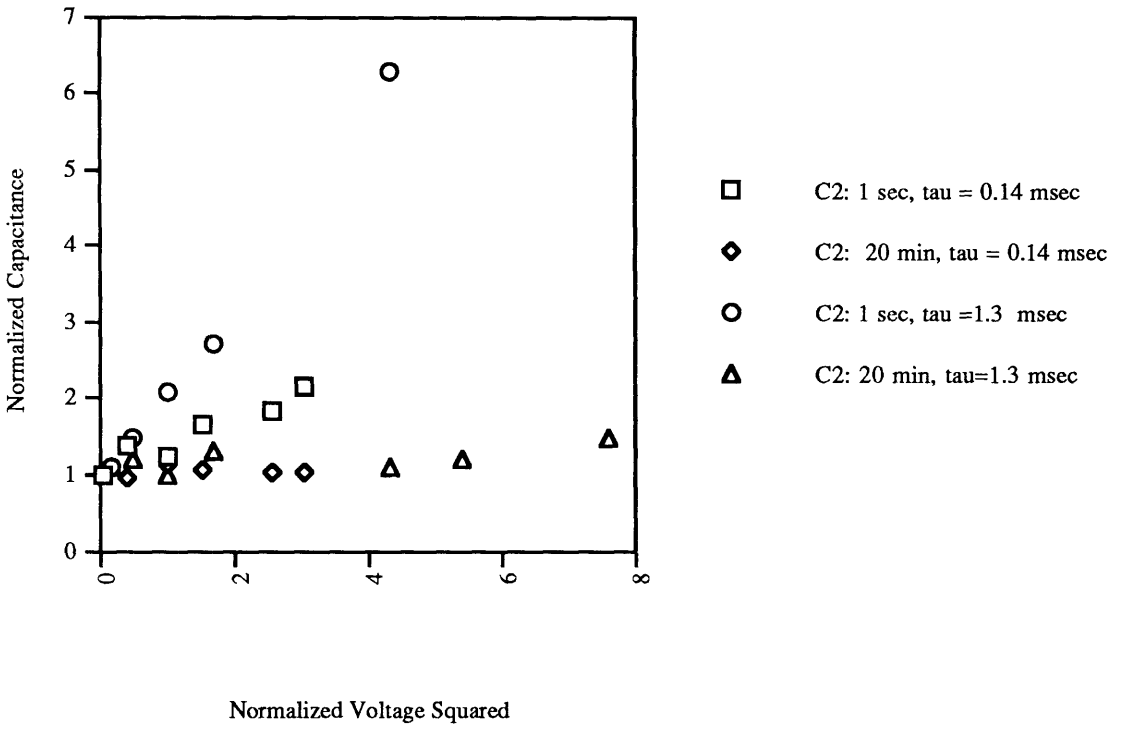

Figure 23: Comparison of the change in C2 for 1.3 msec and 0.14 msec time constants. Capacitance values are normalized to their pre-pulsing value.

4.5 Effects of Multiple Pulses

The pulsing protocol used for the molecular flux experiments described in the introduction, involved pulsing once every five seconds for one hour [7]. One obvious advantage of this strategy is that there is an electrophoretic driving force supplied every five seconds, which should enhance the flux of charged molecules. However, there is another potential advantage, in that the additional pulses may cause a further electroporation of the SC, resulting in the creation of new pores and increased molecular flux. These advantages motivated a study of the impedance changes due to multiple pulses. The studies were performed using the previously

described apparatus, modifying only the software to trigger the pulser at an appropriate interval, and take measurements in between the pulses.

Fig. 24 shows the value of R1 as a function of time for a typical multipulsing experiment. The saw tooth nature of the curves is predicted by the single pulse data. The saw tooth shape arises from the decrease in resistance caused by each pulse, followed by an increase in resistance between pulses. For the 210 and 280 volt cases the steady state level, reached within one minute, is approximately the resistance that would be measured if the skin sample were replaced by saline. It was not possible to reach such a low resistance by the application of a single pulse, even at the highest voltages used. Samples pulsed at lower voltages to not reach such a low resistance, instead the steady state value reached is approximately the same resistance as the plateau reached by a single high voltage pulse.

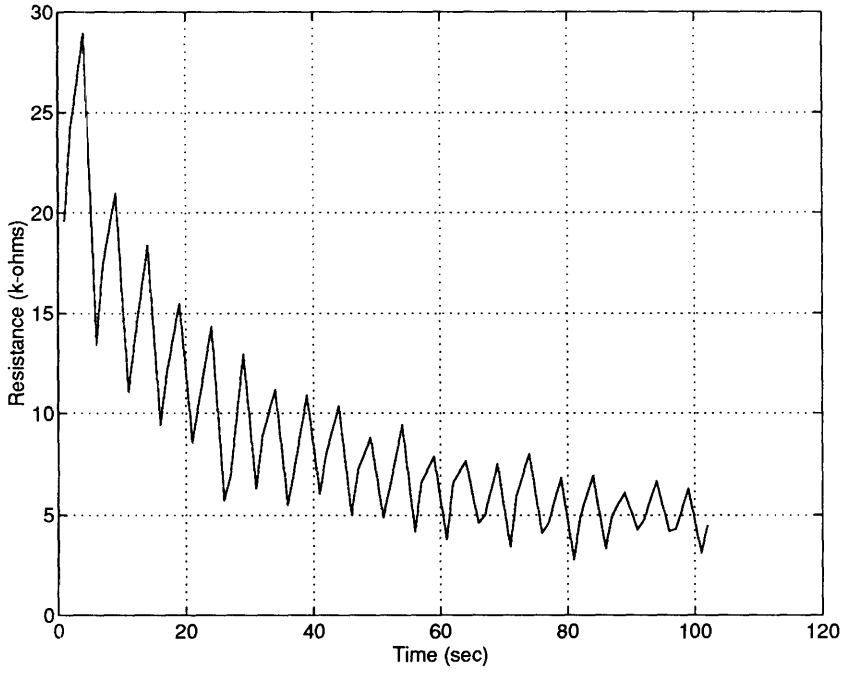

Figure 24: Resistance during a typical multi-pulsing experiment. For the experiment shown, the sample was pulsed once every five seconds at 210 volts.

From the single pulse data, we expect that the recovery between pulses should be well described by a single exponential with a time constant between one and five seconds. This is because the rate of change of the other two recovery time constants (~100 msec and ~ 100 sec) is very small in this region. Fig. 25 shows the recovery time constant in between each pulse for the resistance data shown in fig. 24. The recovery time constant is in the expected region, but displays considerable variability within the range. The variability is similar to the sample-to-sample variation found in the single pulse experiments. It is unlikely that this variation is due solely to measurement error, as each recovery period is well fit to an exponential. This variability over a fixed range suggests that there is may be an underlying stochastic process that leads to the recovery of the conductance. One such possibility is closing of pores, which has been modeled as a stochastic process [17]. As the number of pulses decreases, there is a slight downward trend in the time constant. The decrease in resistance per pulse also decreases with an increasing number of pulses. This is not surprising, since membranes that have already been porated have a higher conductance and it therefore may not possible to develop a large enough transmembrane voltage to create many more pores. The single pulse data shows that the lower pulsing voltages (corresponding to smaller conductance increases one second after the pulse) correlate with smaller recovery time constants.

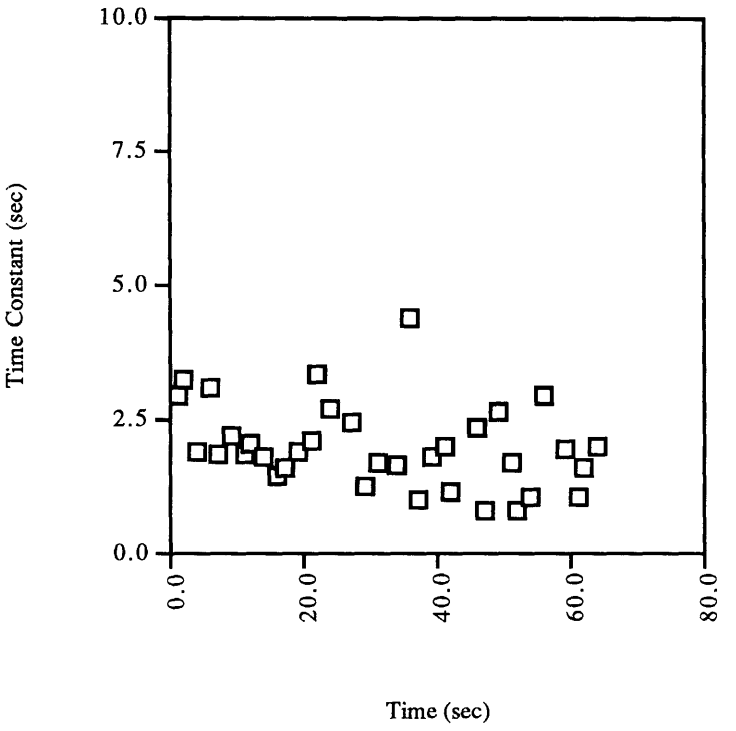

Figure 25: Recovery time constant for data shown in figure 24.

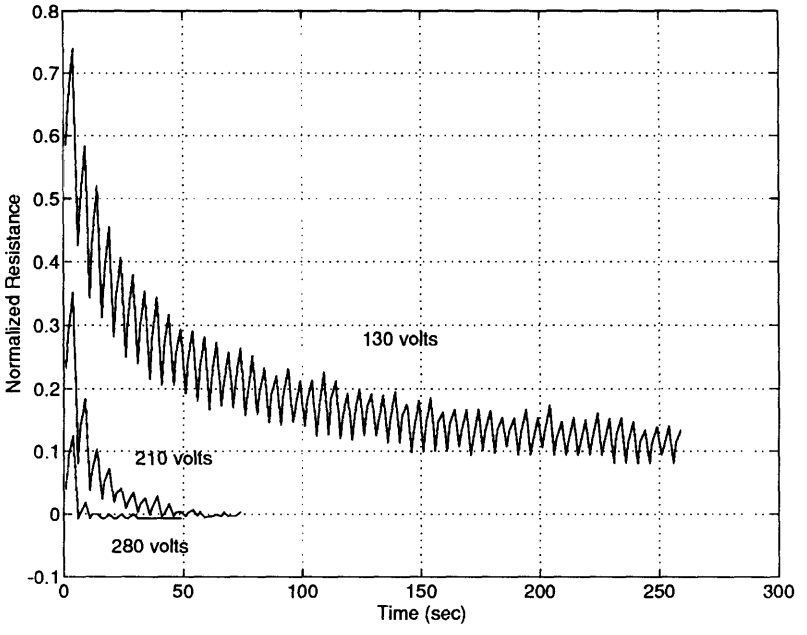

Figure 26: Comparison of multiple pulsing at three different voltages for the same pulsing frequency (1 pulse every 5 seconds).

Figure 27 shows the resistance one second after pulsing as a function of time for two samples pulsed at 210 volts transdermally, with different pulsing frequencies. For the case with the 30 second pulsing period, data were taken for only five seconds after each pulse. A dotted line connects the resistance value at five seconds after pulsing to the resistance value one second after the next pulse. The change due to the first pulse is nearly the same in each case, which is consistent with the single pulse data. For the higher pulsing frequency case, the resistance falls off much more quickly, since the sample is receiving six times as many pulses in a given time, and has less time to recover in between pulses.

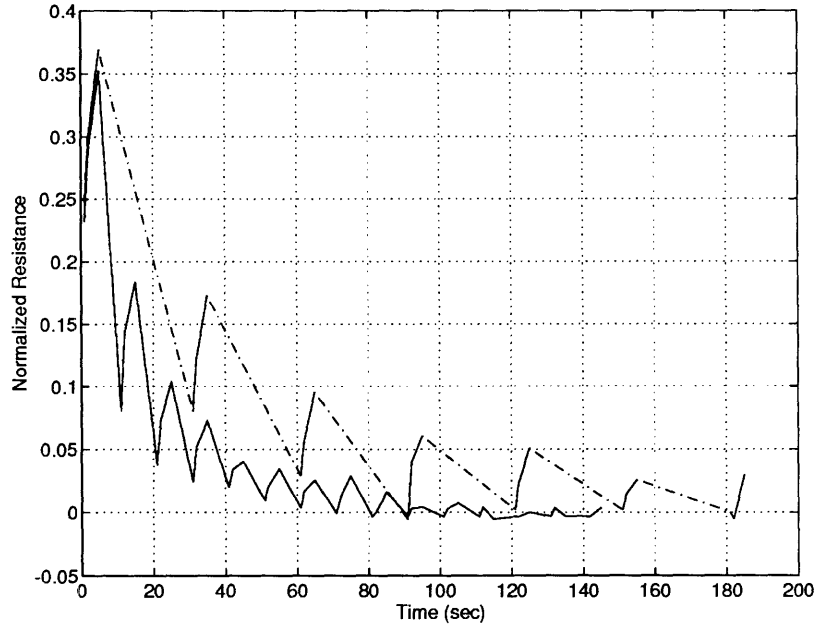

Figure 27: Comparison of multiple pulsing at two different pulsing frequencies for the same voltage (210 volts). Impedance measurements were taken for five seconds after each pulse.

Multiple pulsing also has an effect upon the recovery after pulsing is stopped. For the samples pulsed at a high enough voltage to reach a resistance comparable to that of saline, no significant recovery is present. Samples pulsed at lower voltages exhibit recovery, with three characteristic time constants; $\tau 1$ and $\tau 2$ are in

the same range as the fast time constant found in the single pulse experiment. $\tau 3$ is typically somewhat larger than in the single pulse experiments, by only a factor of two or three. The value to which these samples recover in twenty minutes is lower than the minimum recovery reached in the single pulse experiments in the same time. This is consistent with the hypothesis the further damage results form the passage of current through an already porated membrane.

4.6 Onset of Changes During the Pulse

As mentioned previously, it has been well established that the electrical properties of the skin are non-linear. An exponentially decaying high voltage wave form was chosen so that the results could be compared with the previous data on transdermal fluxes. However, this wave form does not lend itself to a study of the non-linearities of the skin. We can investigate a key feature of electroporation during the pulse: the onset of electroporation on a micro-second time scale, by measuring the current through the skin during a pulse.

The charging time of the skin-chamber system is dominated by the resistance of the bathing saline (~ 400 Ohms) and capacitance of the skin sample (~ 10 nF), and is on the order of a few μsec. In the absence of any changes to the system, the current through the chamber a few μsec after the pulse should be approximately the pulsing voltage divided by the resistance of the skin (recall that the pre-pulsing resistance of the skin is typically 2-4 orders of magnitude greater than that of the chamber plus electrodes).

It was observed, that for lower pulsing voltages, the current wave form closely followed the shape of the applied exponential voltage, but for higher pulsing voltages the shape of the current wave form differed slightly from an exponential decay. However the time scale of these variations was slow compared to the charging time of the skin.

Due to the large range over which the skin resistance varies, a consistent relationship between the transdermal voltage and the current through the skin could not be determined. In general, the current (after the skin charging time) was found to be approximately one order of magnitude higher than expected, in the absence of poration, for low pulsing voltages (< 38 volts for 1.3 msec pulses), and up to four orders of magnitude higher for higher pulsing voltages.

Chapter 5

Discussion

5.1 Comparison of Results with Characteristics of Electroporation

The data present above exhibit many of the characteristics of the electroporation of single bilayers. In both cases there is a decrease in the resistance of the sample within microseconds after application of the of the high voltage. The magnitude of the change increases with voltage and can be either fully or partially reversible. These two cases corresponds directly to two of the four possible outcomes of an electroporation experiment, as outlined earlier.

There is evidence for the fourth possible outcome of electroporation (membrane rupture) from both the single and multiple pulse experiments. The single pulse data in fig. 19 show a sudden decrease in the reversible portion of the change at the same point where the maximum voltage change saturates. If some of the membranes in the SC were to rupture they would not recover, so the abrupt change in the degree of recovery might be explained by membrane rupture. Also, a rupture would create a highly conductive path through the membrane, so trans-membrane voltage would rapidly decrease, and further electroporation would not occur. Thus rupture is a plausible explanation for the saturation of change seen at high voltages in single pulse experiments. For high enough pulsing voltages, the multiple pulse experiments exhibited no significant recovery. consistent with rupture. These experiments also reached a transdermal resistance that was much lower than could be reached by a single pulse. It is reasonable that the additional pulses caused membrane rupture, accounting for both the lower resistance and lack of recovery.

The first outcome, passive charging of the skin capacitance, of an electroporation experiment (a slight increase in conductance of the membrane) was not evident in any of the experiments (the minimum transdermal voltage used was 22 volts, since the Bio-Rad Gene Pulser could not accurately deliver pulses with peak voltages of less than 50 volts). Non-linearities in the skin for voltages much smaller than this have reported in the literature. [25] . Although slight (i.e. less than 10%) conductance changes are observed, they are accompanied by a current during the pulse that is one order of magnitude greater than expected. It has been reported that slight conductance increases occur during the application of iontophoresis [26], which uses much smaller transdermal voltages.

There are a few aspects of the data that differ from the single bilayer results. The experimental results from artificial bilayer membranes show that the electroporation threshold should depend only upon the peak voltage. However a dependence upon the exponential time constant of the pulse was found for skin. Also changes in capacitance were not found in bilayer membranes. It is not too surprising that some differences are found, since the hypothesis is that the SC consists of many bilayers, arranged in series.

To evaluate these differences it is important to first understand the limitations of the circuit model. As stated earlier, the circuit elements R2, C1 and C2 are lumped parameter models of the non-ohmic pathways through the skin, so precise relations between skin structures and these elements cannot be determined. However, we can examine some of the skin structures that contribute to these elements.

The region in between the bilayers is believed to contain very little water [14], so it is reasonable to assume that the resistance in these regions is very high, making the charging time of these bilayers longer compared to the charging time of the skin through saline (typically several microseconds). The branch of the circuit

model containing the series combination of R2 and C2 may in part represent the bilayers and the spaces between them. Typical values for R2 and C2 are on the order of 100 kΩ and 10 nF respectively, with an associated charging time on the order of 1 msec.

As mentioned earlier, the charging time of the skin, which is dominated by the resistance of the saline, is on the order of 1 μsec. However, if the charging time of the bilayers were significantly longer, then it would take much longer for each bilayer to charge. If the charging time for these bilayers were on the order of 1 msec, it would explain the difference in the results for the two exponential time constants. This hypothesis is further strengthened by the fact that the results have the same voltage dependence if the voltage is normalized. Since the bilayers would not charge to the same degree for the shorter time constant pulses, it would take a higher voltage to produce the same level of electroporation.

From previous experimental and theoretical work it has been determined that the electroporation threshold for a single bilayer is approximately one volt, for a pulse on the order of a msec in duration [1-4]. Given that the number of bilayers in the lamellar layers of the SC is about a hundred, the observed results for pulses of a few hundred volts are consistent with the electroporation of single bilayers.

Capacitance changes associated with bilayer electroporation are small (less than 1 or 2%). At lower membrane voltages the capacitance was found to vary with the square of the voltage [27]. This is plausible, since deformation forces that compress the membrane, or that create aqueous pathways (pores), can be expected to depend on spatial gradients of energies. If the material involved (mainly lipids) is polarizable, then these energies and also the forces will have a V^2 dependence. For this general reason the capacitance changes associated with deformation are expected to go as V^2 .

Figure 28 shows the comparison between the conductance change at one second after a pulse and the changes in molecular flux observed by Prausnitz etal. [7]. Here Δ Conductance is the normalized conductivity minus one. This shift was introduced so that zero flux corresponds to zero conductance change. The Calcein flux data was obtained using a 1.3 msec exponential pulse, and the voltage for the 0.14 conductance data has been normalized to the 1.3 msec data by the factor of 0.48 as discussed on page 30. From this data it is clear that there is a linear relationship between electrical conductance and the flux of calcein. This suggests that conductance measurements could be used to predict and control the transdermal flux of moderate size (300 - 1,000 D) charged molecules

There was no a priori reason to expect the flux of a molecule such as calcein to be linearly proportional to the change in electrical conductance measured one second after the pulse. The flux depends on the permeability of the skin to the molecule and the magnitude of the electrical driving force. The conductance is a measure of the permeability of the skin to sodium and chloride ions, and is itself independent of voltage (i.e. driving force) for the small (< 2 Å) currents used to measure the impedance. Furthermore, the calcein transport occurs primarily during the multiple high voltage pulse due to the large driving force they supplies. The electrical conductance is measured a full second after a single pulse. In spite of these different conditions, there is a striking agreement between these measurements.

Sodium and chloride ions, the dominant carriers of current, cross the skin primarily through aqueous pathways. Since the flux and conductance curves have the same general dependence upon voltage, it is likely that the increased transport of calcein is primarily through aqueous pathways. The hypothesized electroporation of the lipid bilayers of the skin would create aqueous pathways through a region that contained little or no water prior to electroporation.

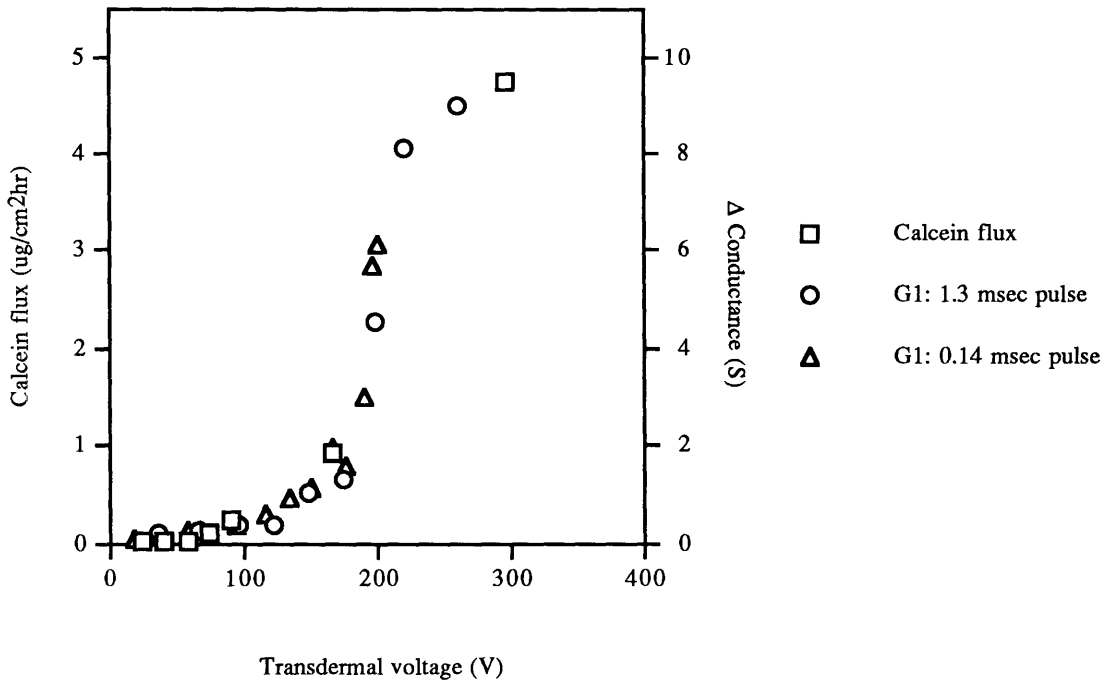

Figure 28: Comparison of the calcein flux and conductivity changes due to electroporation. Δ conductance is the normalized conductivity minus one, this shift is made so that zero flux corresponds to zero conductance change. The calcein flux data was obtained using a 1.3 msec exponential pulse, and the voltage for the 0.14 conductance data has been normalized to the 1.3 msec data by the factor of .48 as discussed on page 30.

5.2 Future Work

5.2.1 Further Investigations into Tissue Electroporation

Many variables in these experiments were fixed, so that the results could be directly compared to the flux studies and to limit the scope of work. Impedance studies are faster and easier to carry out than molecular flux experiments, so impedance measurements can be used to determine if a set of variables is worth investigating with a subsequent full study involving the flux of many molecules. Some examples of some of these variables are the time dependence of the

high voltage wave form (e.g. square wave or ramp), temperature, and high voltage electrode material.

Several of the studies presented here are simply initial investigations, and the results certainly warrant further research. Particularly more complete studies of the multiple pulse and variation of time constant experiments could lead to interesting insight into both the molecular flux results and the nature of the changes occurring within the skin.

Finally, a full study of the non-linearities in the voltage - current relationship could yield very valuable insight into the changes occurring within the skin. For such a study, a high voltage pulser, preferably programmable, capable of producing several different wave forms. Both current and voltage sources should be used to fully characterize the non-linearities.

5.2.2 Other Applications of the Skin Impedance Measurement System

Electroporation is only one of several candidate mechanisms for enhancing transdermal drug delivery. Other possibilities include iontophoresis , chemical enhancers and ultrasound [13, 14]. Electrical impedance measurements could provide a simple, quick way of evaluating and comparing different methods.

As an example of the flexibility of the system described in this thesis, changes in impedance during the application of ultrasound were measured. The ultrasound was turned off momentarily while the measurements were made, since it was determined that the presence of ultrasound affected the electrical measurements. Also, there was some heating due to the ultrasound, but the temperature rise of 2 - 5^{o}C alone was not enough to account for the observed changes in resistance. (The variation of skin resistance due to temperature was found to be approximately -3% per degree C, which

agrees well with the literature [28]). Fig. 29 shows the impedance changes due to ultrasound. Again a decrease in electrical resistance is evident, but on a slower time scale than electroporation. After the application of ultrasound is terminated, the impedance returned towards its initial value. Further studies will have to be done to determine the dynamics of the changes and recovery due to the application of ultrasound.

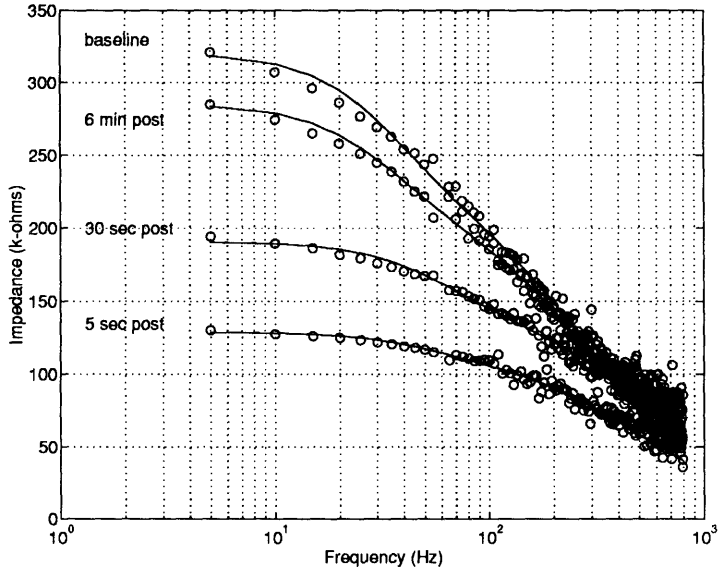

Figure 29: Impedance changes due to the application of Ultrasound.

Chapter 6

Summary

As stated at the outset of this thesis, the two primary goals were: 1) to carry out electrical impedance measurements which would partially test the hypothesis that "high voltage" pulses cause electroporation of the SC, and 2) to relate the changes in electrical impedance to the previously observed changes in the transdermal flux of certain molecules under similar conditions

The changes in the electrical properties of human skin due to high voltage pulsing demonstrate two important characteristics of electroporation. A large decrease in the resistance within a few microseconds after the application of the high voltage pulse and three of the four characteristic types of characteristic electrical behavior found in the electroporation of planar bilayer membranes. For pulsed skin this behavior consists of: 1) low voltage pulsing resulting in conductivity increases that are completely reversible, 2) somewhat higher pulsing voltages causing resistance changes which are irreversible, and 3) and even higher voltages resulting in the changes that saturate, possibly as a result of membrane rupture, and an associated persistent low resistance state.

The changes in electrical conductance of the skin were found to be proportional to the previously observed changes in molecular flux across the skin. This result has important implications for the closed-loop control of transdermal drug delivery by electroporation, as it suggests the rapid electrical assessment of electrically pulsed skin may give sufficient real-time information to allow electrically controlled drug delivery. Furthermore it indicates that the increased transport of calcein is probably due to aqueous pathways created by electroporation.

Bibliography

1. Neumann, E., Sowers, A. E. and Jordan, C. A., *Electroporation and electrofusion in cell biology*, Plenum Press, New York, 1989.

2. Chang, D. C., Chassy, B. M., Saunders, J. A. and Sowers, A. E.s, *Guide to electroporation and electrofusion*, Academic Press, New York, 1992.

3. Orlowski, S. and Mir, L. M., Cell electropermeabilization: a new tool for biochemical and pharmacological studies, *Biochim. Biophys. Acta*, 1154, 51-63, 1993.

4. Weaver, J. C., Electroporation: a general phenomenon for manipulating cells and tissues, *J. Cell. Biochem.*, 51, 426-435, 1993.

5. Prausnitz, M. R., Bose, V. G., Langer, R. and Weaver, J. C., Transdermal drug delivery by electroporation, *Proceed. Intern. Symp. Control. Rel. Bioact. Mater.*, 19, 232-233, 1992.

6. Bommannan, D., Leung, L., Tamada, J., Sharifi, J., Abraham, W. and Potts, R., Transdermal delivery of luteinizing hormone releasing hormone: comparison between electroporation and iontophoresis in vitro, *Proceed. Intern. Symp. Control. Rel. Bioact. Mater.*, 20, 97-98, 1993.

7. Prausnitz, M. R., Bose, V. G., Langer, R. and Weaver, J. C., Electroporation of mammalian skin: a mechanism to enhance transdermal drug delivery, *Proc. Natl. Acad. Sci. USA*, 90, 10504-10508, 1993.

8. Okino, M. and Mohri, H., Effects of a high voltage electrical impulse and an anticancer drug on *in vivo* growing tumors, *Jpn. J. Cancer Res.*, 78, 1319-1321, 1987.

9. Mir, L. M., Orlowski, S., Belehradek, J. and Paoletti, C., Electrochemotherapy: potentiation of antitumor effect of bleomycin by local electric pulses, *Eur. J. Cancer*, 27, 68-72, 1991.

10. Salford, L. G., Persson, B. R. R., Brun, A., Ceberg, C. P., Kongstad, P. C. and Mir, L. M., A new brain tumour therapy combining bleomycin with in vivo electropermeabilization, *Biochem. Biophys. Res. Com.*, 194, 938-943, 1993.

11. Benz, R. F., Beckers, F. and Zimmermann, U., Reversible electrical breakdown of lipid bilayer membranes: a charge-pulse relaxation study, *J. Membrane Bio.*, 48, 181-204, 1979.

12. Abidor, I. G., Arakelyan, V. B., Chernomordik, L. V., Chizmadzhev, Y. A., Pastushenko, V. F. and Tarasevich, M. R., Electric breakdown of bilayer membranes: I. the main experimental facts and their qualitative discussion, *Bioelectrochem. Bioenerget.*, 6, 37-52, 1979.

13. Bronaugh, R. L. and Maibach, H. I., Bronaugh, R. L. and Maibach, H. I.s, *Percutaneous absorption, mechanisms -- methodology -- drug delivery*, 6, Marcel Dekker, New York, 1989.

14. Hadgraft, J. and Guy, R. H., Hadgraft, J. and Guy, R. H.s, *Transdermal drug delivery: developmental issues and research initiatives*, 35, Marcel Dekker, New York, 1989.

15. Gray, H., *Gray's Anatomy*, 36, W.B. Saunders Company, Philadelpia, Pa, 198.

16. Elias, P. M., Epidermal barrier function: intercellular lamellar lipid structures, origin, composition and metabolism, *J. Controlled Release*, 15, 199-208, 1991.

17. Barnett, A. and Weaver, J. C., A unified, quantitative theory of reversible electrical breakdown and rupture, *Bioelectrochem. and Bioenerg.*, 25, 163-182, 1991.

18. Cullander, C. and Guy, R. H., Transdermal delivery of peptides and proteins, *Adv. Drug Deliv. Rev.*, 8, 291-329, 1992.

19. Vigouroux, R., Sur le role de la resistance electrique des tissus dans l'electrodiagnostic., *Comptes rendus des Seancs de la Societe de Biologie*, 31, 336-339, 1879.

20. Rosell, J., Colominas, J., Riu, P., Pallas-Areny, R. and Webster, J. G., Skin impedance from 1 Hz to 1 MHz, *IEEE Trans. Biomed. Eng.*, 35, 649-651, 1988.

21. Fere, C., Note sur les modifications de la tension electrique la corps humain., *Comptes rendus des Seancs de la Societe de Biologie*, 5, 28-33, 1888.

22. Salter, D. C. and Phil, D., Evaluating skin preparations using in vivo electrical measurements, 1982.

23. Yamamoto, T. and Yamamoto, Y., Electrical properties of the epidermal stratum corneum, *Med. & Biol. Eng.*, 151-158, 1976.

24. Gummer, C. L., *The in vitro evaluation of transdermal delivery*, Transdermal drug delivery: development issues and research initiatives, 35, J. Hadgraft and R. H. Guy, Marcel Dekker, New York, 1989, 177-186.

25. Yamamoto, T. and Yamamoto, Y., Non-linear electrical properties of skin in the low frequency range, *Med. & Biol. Eng. & Comput.*, 19, 302-310, 1981.

26. Burnette, R. R. and Bagniefski, T. M., Influence of constant current iontophoresis on the impedance and passive Na+

permeability of excised nude mouse skin, *J. Pharm. Sci.*, 77, 492-497, 1988.

27. Alvarez, R. L. O., Voltage Dependent Capacitance in Lipid Bilayers made from Monolayers, *Biophys. J.*, 21, 1 - 17, 1978.

28. Edelberg, R., *Electrical Activity of the Skin*, Handbook of Physiology, R. S. N. Greenfield, Holt, Rinehart and Winston Inc., New York, 1972,

Appendix A: Hardware

Cicuit diagram for impedance measurement system.

- includes impedance measurmente system, computer interface and connections to Bio-Rad Gene Pulser

Impedance Measurement System

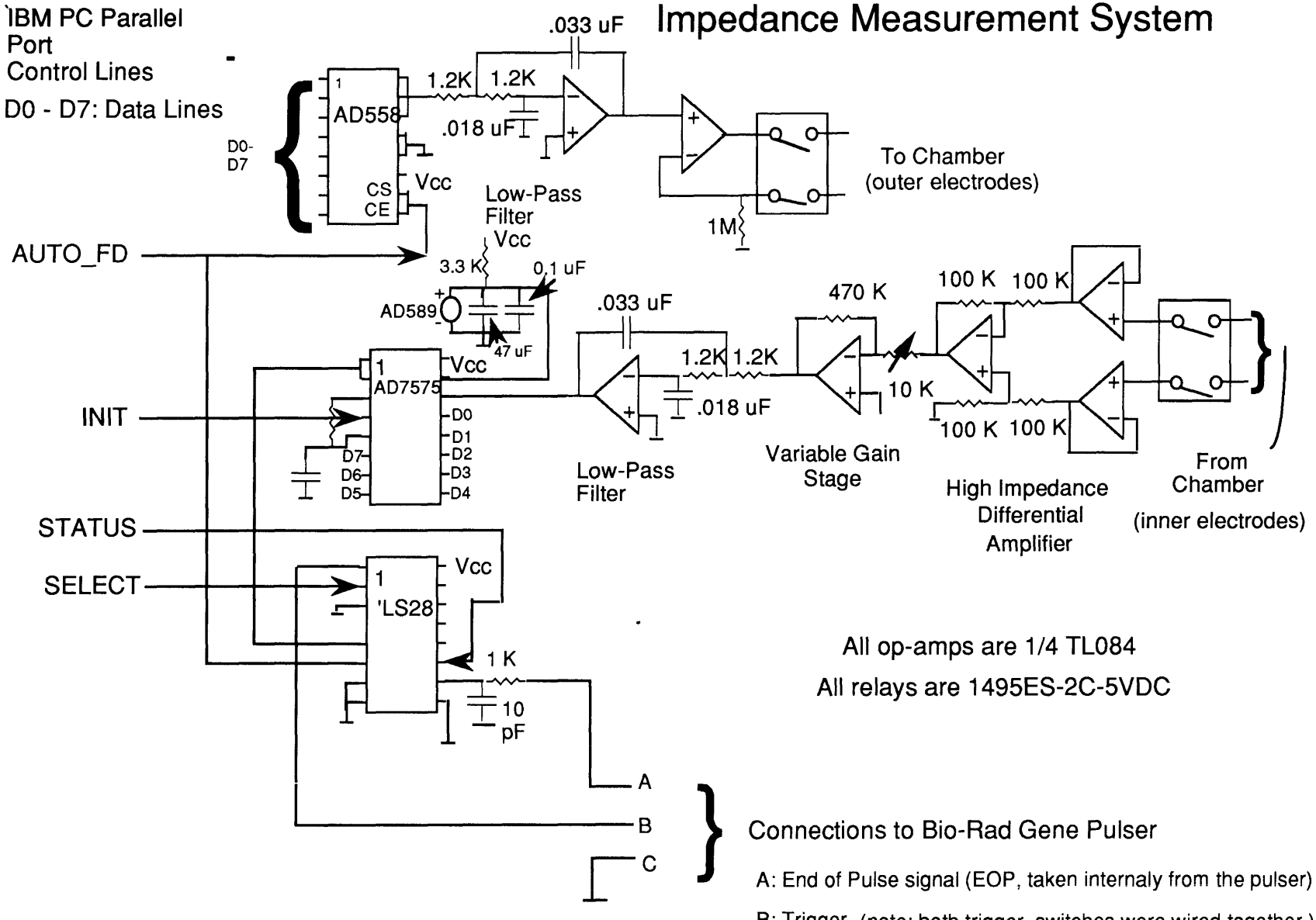

All op-amps are 1/4 TL084

All relays are 1495ES-2C-5VDC

Connections to Bio-Rad Gene Pulser

A: End of Pulse signal (EOP, taken internaly from the pulser)

B: Trigger (note: both trigger switches were wired together)

C: Ground

Appendix B: Software

Contents:

B.1 Turbo C++ code for data acquisition 486 based platform.

B.1.1) exp.c

- Impedance measurement experiemental control, and data acquitsition software.

B.1.2) hppulse.c

- HP oscilloscope interface software:program makes an impedance measurement, triggers a high voltage pulse, makes another impedance measurment after the pulse, then downloads the waveform corresponding to current during the pulse from the HP scope.

B.2 Matlab code for data analysis.

B.2.1 Function datafit.m, analyzes data files from 486.

B.2.2 Subroutine dofit.m performs fourier transform and

-calls fitting routin

B2.3 Subroutine labfit1z2p.m

- Calls least sq. funtion for a fit to 1 zero and 2 poles

B2.4 f1z2p.m

- function pased to least squares routine which returns error between the current fit and the data

BI. Turbo C++ code for data acquisition 486 based platform.

B1.1. exp.c

```
#include <stdio.h>
#include <stdlib.h>
#include <math.h>
#include <bios.h>
#include <time.h>
#include <dos.h>
#include <float.h>
#include <io.h>
#include <fcntl.h>
#include <sys\stat.h>



#define DATAPOINTS 1000
#define FASTDATAPOINTS 20
#define FASTMEASUREMENTS 90
#define MEASUREMENTS 18
#define PRINTER_DATA_PORT 0x0378
#define PRINTER_STATUS_PORT 0x0379
#define PRINTER_CONTROL_PORT 0x037a

#define PRINTER_STROBE_LO_CODE 0x05
#define PRINTER_AUTOFD_HI_CODE 0x04
#define PRINTER_AUTOFD_LO_CODE 0x06
#define PRINTER_SELECT_LO_CODE 0x0c
#define PRINTER_SELECT_HI_CODE 0x04
#define PRINTER_NEUTRAL_CODE 0x0c
#define PRINTER_INIT_CODE 0x08

#define PRINTER_DATA_WRITE 0x04
#define PRINTER_DATA_READ 0x24

#define WRITE_MODE (PRINTER_AUTOFD_HI_CODE | PRINTER_DATA_WRITE |
PRINTER_SELECT_LO_CODE)

#define READ_MODE  (PRINTER_AUTOFD_LO_CODE | PRINTER_DATA_READ |
PRINTER_SELECT_LO_CODE)

void measure(int argc,unsigned char *dcptr,unsigned char *dataptr,int
current_value,FILE *outfileptr)

{
        int j,m,dcavg;
        unsigned char *dcbase,*database;
        dcbase = dcptr;
```

```
        database = dataptr;


        outportb(PRINTER_CONTROL_PORT,READ_MODE);
        for(m=0;m<5;m++)
        {
                *dcptr = inport(PRINTER_DATA_PORT);
                dcptr++;
                for(j=0;j<305;j++)
                        ;
        }

        for (m=0;m<DATAPOINTS;m++)
        {
                outportb(PRINTER_CONTROL_PORT,WRITE_MODE);
                outportb(PRINTER_DATA_PORT,current_value);
                outportb(PRINTER_CONTROL_PORT,PRINTER_INIT_CODE);
                outportb(PRINTER_CONTROL_PORT,PRINTER_NEUTRAL_CODE);
                outportb(PRINTER_CONTROL_PORT,READ_MODE);
                for (j=0;j<305;j++)
                        ;
                *dataptr = inport(PRINTER_DATA_PORT);
                dataptr++;
        }

        outportb(PRINTER_CONTROL_PORT,WRITE_MODE);
        outportb(PRINTER_DATA_PORT,0);
        outportb(PRINTER_CONTROL_PORT,PRINTER_INIT_CODE);
        for (j=0;j<40;j++)
                ;
        outportb(PRINTER_CONTROL_PORT,PRINTER_NEUTRAL_CODE);
        for (j=0;j<40;j++)
                        ;

        dcptr = dcbase;
        dcptr++;
        dataptr = database;
        dcavg = 0;
        for (m=1;m<5;m++)
        {
                dcavg = dcavg + *dcptr;
                dcptr++;
        }

        dcavg = (int) ((float) dcavg / 4.0);
//      printf("dc offset = %d\n\n",dcavg);

        /* Write data to file if a filename was given */
        if (argc == 5)
        {
                for (j=0;j<DATAPOINTS;j++)
                {
                        fprintf(outfileptr,"%d\n",*dataptr-dcavg);
                        dataptr++;
```

```
                }
        }
}

void fastmeasure(int argc,unsigned char *dataptr,int current_value,FILE *outfileptr)
{
        int j,n,m,current;
        unsigned char *database;
        time_t time1;

        database = dataptr;

        outportb(PRINTER_CONTROL_PORT,READ_MODE);
        for (n=0;n<FASTMEASUREMENTS;n++)
        {
        current = current_value;
                for (m=0;m<FASTDATAPOINTS;m++)
                        {
                          outportb(PRINTER_CONTROL_PORT,WRITE_MODE);
                          outportb(PRINTER_DATA_PORT,current);
                         outportb(PRINTER_CONTROL_PORT,PRINTER_INIT_CODE)
                 outportb(PRINTER_CONTROL_PORT,PRINTER_NEUTRAL_CODE);
                          outportb(PRINTER_CONTROL_PORT,READ_MODE);
                          for (j=0;j<305;j++)
                                  ;
                          *dataptr = inport(PRINTER_DATA_PORT);
                          dataptr++;
                 }
                 current = 0;
                 outportb(PRINTER_CONTROL_PORT,WRITE_MODE);
                 outportb(PRINTER_DATA_PORT,current);
                 outportb(PRINTER_CONTROL_PORT,PRINTER_INIT_CODE);

        outportb(PRINTER_CONTROL_PORT,PRINTER_NEUTRAL_CODE);

                  for (j=0;j<7;j++)
                          time(&time1);
          }
        outportb(PRINTER_CONTROL_PORT,WRITE_MODE);
        outportb(PRINTER_DATA_PORT,0);
        outportb(PRINTER_CONTROL_PORT,PRINTER_INIT_CODE);
        for (j=0;j<40;j++)
                ;
        outportb(PRINTER_CONTROL_PORT,PRINTER_NEUTRAL_CODE);
        for (j=0;j<40;j++)
                ;

        dataptr = database;
        /* Write data to file if a filename was given */
        if (argc == 5)
        {
//              printf("writing fast data\n");

                for (j=0;j<FASTDATAPOINTS*FASTMEASUREMENTS;j++)
```

```
                {
//                      printf("%d, fastdata = %d\n",j,*dataptr);
                        fprintf(outfileptr,"%d\n",*dataptr);
                        dataptr++;
                }
        }
}

void pulse(void)
{
        int j;
        unsigned char status;

        /* Wait Until Pulser is Ready */
        do{
                status = inport(PRINTER_STATUS_PORT) & 128;
                printf("wait status = %d\n",status);
        }while(status < 128);

        /* Trigger Pulser */
        outportb(PRINTER_CONTROL_PORT,PRINTER_SELECT_LO_CODE);
        for (j=1;j<20;j++)
                ;
        outportb(PRINTER_CONTROL_PORT,PRINTER_SELECT_HI_CODE);
        printf("Pulser Triggered\n");

        /* Wait for end of Pulse */
        do{
                status = inport(PRINTER_STATUS_PORT) & 128;
//              printf("status = %d\n",status);
        }while(status > 127);
}

void main(int argc, char **argv)
{
        int m,i,j,current_value,cv;
        unsigned char data[DATAPOINTS], dc[5],
fdata[FASTMEASUREMENTS*FASTDATAPOINTS];
        float gain,current,delaypre_cur;
        double meas_time[MEASUREMENTS];
        time_t time_zero,time1;
        FILE *out;

        /* Define Measurement Times */

        meas_time[1] = 1;
        meas_time[2] = 2;
        meas_time[3] = 5;
        meas_time[4] = 10;
        meas_time[5] = 20;
        meas_time[6] = 30;

        for(m=7;m <= 16;m++)
                meas_time[m]=60*(m-6);
```

```
        for(m=16;m <= MEASUREMENTS;m++)
                meas_time[m]=10*60*(m-15);

        if (argc > 5 || argc < 2)
        {
                printf("Usage: exp3 current(uA) post_current(uA) gain filename\n");
                exit(0);
        }

        sscanf(argv[2],"%f",&current);
        sscanf(argv[1],"%f",&pre_cur);
        current = 255*current/2.89;
        pre_cur = 255*pre_cur/2.89;
//      printf("current value = %f, %d\n",current,(int) current);
        outportb(PRINTER_CONTROL_PORT,WRITE_MODE);
        outportb(PRINTER_DATA_PORT,0);

        /* Open data file if a filename was given */
        if (argc == 5)
        {
                sscanf(argv[3],"%f",&gain);
//              printf("gain = %f\n",gain);
                if((out = fopen(argv[4],"wt")) == NULL)
                {
                        printf("Error opening output file");
                        exit(0);
                }
                fprintf(out,"%d\n",DATAPOINTS);
                fprintf(out,"%f\n",gain);
                cv = (int) pre_cur;
                printf("cv = %d \n",cv);
                current_value = (int) current;
                fprintf(out,"%d\n",cv);
                printf("current_value = %d \n",current_value);
                fprintf(out,"%d\n",current_value);
                fprintf(out,"%d\n",MEASUREMENTS);
                fprintf(out,"%d\n",FASTMEASUREMENTS);
                fprintf(out,"%d\n",FASTDATAPOINTS);
                for(m=1;m<=MEASUREMENTS;m++)
                        fprintf(out,"%f\n",meas_time[m]);
        }

        measure(argc,dc,data,cv,out);
        pulse();
        time(&time_zero);
        printf("Pulse finished\n");
        outportb(PRINTER_CONTROL_PORT,WRITE_MODE);
//      outportb(PRINTER_DATA_PORT,0);

        printf("End of pulse detected\n\n");
        fastmeasure(argc,fdata,current_value,out);
        printf("Fast measurements completed\n");
```

```
//      Delay until measurement at 1 second
        for(i=1;i<275;i++)
                time(&time1);
        measure(argc,dc,data,current_value,out);

//      Delay until measurement at 2 seconds
        for(i=1;i<1230;i++)
                time(&time1);
        measure(argc,dc,data,current_value,out);

//      Delay until measurement at 5 seconds
        for(i=1;i<(1230+2*1550);i++)
                time(&time1);
        measure(argc,dc,data,current_value,out);

//      Delay until measurement at 10 seconds
        for(i=1;i<4*1550+1230;i++)
                time(&time1);
        measure(argc,dc,data,current_value,out);

//      Delay until measurement at 15 seconds
        for(i=1;i<4*1550+1230;i++)
                time(&time1);
        measure(argc,dc,data,current_value,out);

//      Delay until measurement at 20 seconds
        for(i=1;i<4*1550+1230;i++)
                time(&time1);
        measure(argc,dc,data,current_value,out);
//      Delay until measurement at 25 seconds
        for(i=1;i<4*1550+1230;i++)
                time(&time1);
        measure(argc,dc,data,current_value,out);
//      Delay until measurement at 30 seconds
        for(i=1;i<4*1550+1230;i++)
                        time(&time1);
        measure(argc,dc,data,current_value,out);

        for(m=1;m<MEASUREMENTS-6;m++)
        {
                do{
                        time(&time1);
//              printf("%f,%f\n",meas_time[m],difftime(time1,time_zero));
                }while(meas_time[m+6] > difftime(time1,time_zero));
                printf("Measurement at %f min completed\n",meas_time[m+6]/60.0);
                measure(argc,dc,data,current_value,out);
        }
        fclose(out);
}
```

B1.2 hpulse.c

```
#include <stdio.h>
#include <bios.h>
#include <time.h>

#define COM1  0
#define COM2  1
#define ACQ_POINTS 800

/* Communications parameters 9600 Baud, No parity, 1 stop bit, 8 data bits) */
#define SETTINGS (0xE0 | 0x00 | 0x00 | 0x03)

#define DATAPOINTS 1000
#define FASTDATAPOINTS 20
#define FASTMEASUREMENTS 90
#define MEASUREMENTS 1
#define PRINTER_DATA_PORT 0x0378
#define PRINTER_STATUS_PORT 0x0379
#define PRINTER_CONTROL_PORT 0x037a
#define PRINTER_STROBE_LO_CODE 0x05
#define PRINTER_AUTOFD_HI_CODE 0x04
#define PRINTER_AUTOFD_LO_CODE 0x06
#define PRINTER_SELECT_LO_CODE 0x0c
#define PRINTER_SELECT_HI_CODE 0x04
#define PRINTER_NEUTRAL_CODE 0x0c
#define PRINTER_INIT_CODE 0x08

#define PRINTER_DATA_WRITE 0x04
#define PRINTER_DATA_READ 0x24

#define WRITE_MODE (PRINTER_AUTOFD_HI_CODE | PRINTER_DATA_WRITE |
PRINTER_SELECT_LO_CODE)

#define READ_MODE  (PRINTER_AUTOFD_LO_CODE | PRINTER_DATA_READ |
PRINTER_SELECT_LO_CODE)

void measure(int argc,unsigned char *dcptr,unsigned char *dataptr,int
current_value,FILE *outfileptr)
{
        int j,m,dcavg;
        unsigned char *dcbase,*database;

        dcbase = dcptr;
```

```
        database = dataptr;

        outportb(PRINTER_CONTROL_PORT,READ_MODE);
        for(m=0;m<5;m++)
        {
                *dcptr = inport(PRINTER_DATA_PORT);
                dcptr++         ;
                for(j=0;j<305;j++)
                        ;
        }

        for (m=0;m<DATAPOINTS;m++)
        {
                outportb(PRINTER_CONTROL_PORT,WRITE_MODE);
                outportb(PRINTER_DATA_PORT,current_value);
                outportb(PRINTER_CONTROL_PORT,PRINTER_INIT_CODE);
                outportb(PRINTER_CONTROL_PORT,PRINTER_NEUTRAL_CODE);
                outportb(PRINTER_CONTROL_PORT,READ_MODE);
                for (j=0;j<305;j++)
                        ;
                *dataptr = inport(PRINTER_DATA_PORT);
                dataptr++;
        }

        outportb(PRINTER_CONTROL_PORT,WRITE_MODE);
        outportb(PRINTER_DATA_PORT,0);
        outportb(PRINTER_CONTROL_PORT,PRINTER_INIT_CODE);
        for (j=0;j<40;j++)
                ;

        outportb(PRINTER_CONTROL_PORT,PRINTER_NEUTRAL_CODE);
        for (j=0;j<40;j++)
                        ;

        dcptr = dcbase;
        dcptr++;
        dataptr = database;
        dcavg = 0;
        for (m=1;m<5;m++)
        {
                dcavg = dcavg + *dcptr;
                dcptr++;
        }

        dcavg = (int) ((float) dcavg / 4.0);
//      printf("dc offset = %d\n\n",dcavg);
```

```
        /* Write data to file if a filename was given */
        if (argc == 4)
        {
                for (j=0;j<DATAPOINTS;j++)
                {
                        fprintf(outfileptr,"%d\n",*dataptr-dcavg);
                        dataptr++;
                }
        }
}

void fastmeasure(int argc,unsigned char *dataptr,int current_value,FILE *outfileptr)
{
        int j,n,m,current;
        unsigned char *database;
        time_t time1;

        database = dataptr;

        outportb(PRINTER_CONTROL_PORT,READ_MODE);
        for (n=0;n<FASTMEASUREMENTS;n++)
        {
        current = current_value;
                for (m=0;m<FASTDATAPOINTS;m++)
                        {
                          outportb(PRINTER_CONTROL_PORT,WRITE_MODE);
                          outportb(PRINTER_DATA_PORT,current);
                         outportb(PRINTER_CONTROL_PORT,PRINTER_INIT_CODE);

                  outportb(PRINTER_CONTROL_PORT,PRINTER_NEUTRAL_CODE);
                          outportb(PRINTER_CONTROL_PORT,READ_MODE);
                          for (j=0;j<305;j++)
                                  ;
                          *dataptr = inport(PRINTER_DATA_PORT);
                          dataptr++;
                  }
                  current = 0;
                  outportb(PRINTER_CONTROL_PORT,WRITE_MODE);
                  outportb(PRINTER_DATA_PORT,current);
                  outportb(PRINTER_CONTROL_PORT,PRINTER_INIT_CODE);

outportb(PRINTER_CONTROL_PORT,PRINTER_NEUTRAL_CODE);

                  for (j=0;j<7;j++)
                          time(&time1);
```

```
        }
        outportb(PRINTER_CONTROL_PORT,WRITE_MODE);
        outportb(PRINTER_DATA_PORT,0);
        outportb(PRINTER_CONTROL_PORT,PRINTER_INIT_CODE);
        for (j=0;j<40;j++)
                ;
        outportb(PRINTER_CONTROL_PORT,PRINTER_NEUTRAL_CODE);
        for (j=0;j<40;j++)
                ;

        dataptr = database;

        /* Write data to file if a filename was given */
        if (argc == 4)
        {
//              printf("writing fast data\n");

                for (j=0;j<FASTDATAPOINTS*FASTMEASUREMENTS;j++)
                {
//                      printf("%d, fastdata = %d\n",j,*dataptr);
                        fprintf(outfileptr,"%d\n",*dataptr);
                        dataptr++;
                }
        }
}

void pulse(void)
{
        int j;
        unsigned char status;

        /* Wait Until Pulser is Ready */
        do{
                status = inport(PRINTER_STATUS_PORT) & 128;
                printf("wait status = %d\n",status);
        }while(status < 128);

        /* Trigger Pulser */
        outportb(PRINTER_CONTROL_PORT,PRINTER_SELECT_LO_CODE);
        for (j=1;j<20;j++)
                ;
        outportb(PRINTER_CONTROL_PORT,PRINTER_SELECT_HI_CODE);
        printf("Pulser Triggered\n");

        /* Wait for end of Pulse */
        do{
```

```
                status = inport(PRINTER_STATUS_PORT) & 128;
//              printf("status = %d\n",status);
        }while(status > 127);
}

long hpsend(char *cmd,int d_time)
{
        int i,j,length,dummy;
        long status;

        length = strlen(cmd);
//      printf("string length = %d\n",length);
        for (i=1 ; i < length+1 ; i++)
        {
                status=bioscom(1,*cmd,COM2);
                ++cmd;
                delay(1);
        }

//      Delay for scope to process command
        delay(d_time);
        return(status);
}

void hpget(int *dataptr,int num_data)
{
        int i;
        int status;

        for(i=1;i<num_data+1;i++)
        {

// Wait for Data Set ready flag
        do{
                status=bioscom(2,0,COM2);
//                      printf("status = %d    Data Ready = %d\n",status,(status &&
256));
                        }while((status && 256) < 0);
//              status=bioscom(2,0,COM2);
//              printf("i=%d,    status=%d\n",i,status);
                *dataptr=status;
                ++dataptr;
        }
}

void initialize(void)
```

```
{
        int i;

//      Set COM2 to 9600 Baud, 1 stop bit, no parity
        bioscom(0,0xE3,COM2);

//      Channel 1 settings
        hpsend("*RST\n",1000);
        hpsend("*RCL 10\n",300);
        hpsend(":DITH OFF\n",1);
/*
        hpsend(":CHAN1:PROB X10\n",1);
        hpsend(":CHAN1:RANG 40 V\n",1);
        hpsend(":CHAN2:PROB X10\n",1);
        hpsend(":CHAN2:RANG 40 V\n",1);
 */
//      Trigger settings
//      hpsend(":TRIG:MODE NORM\n",1000);
//      hpsend(":TRIG:LEV 1\n",1);

}

void wait_for_trig()
{
        int i,reply;
        unsigned char answer;

        hpsend(":TER?\n",1);
        do{
                reply=bioscom(2,0,COM2);
        printf("trigger = %d\n",reply);
        }while((reply && 256) == 0);
        printf("trigger = %d\n",reply);
}

void main(int argc, char **argv)
{
        int m,i,j,current_value,answer[2500];
        unsigned char
data[DATAPOINTS],dc[5],fdata[FASTMEASUREMENTS*FASTDATAPOINTS];
        float gain,current,delay,r1,r2,avg;
        time_t time_zero,time1;
        double meas_time;
        FILE *out;

        /* Define Measurement Times */
```

```
        meas_time = 1;

        if (argc > 4 || argc < 2)
        {
                printf("Usage: meas current(uA) delay\n");
                exit(0);
        }

        sscanf(argv[1],"%f",&current);
        current = 255*current/2.89;
//      printf("current value = %f, %d\n",current,(int) current);
        outportb(PRINTER_CONTROL_PORT,WRITE_MODE);
        outportb(PRINTER_DATA_PORT,0);

        /* Open data file if a filename was given */
        if (argc == 4)
        {
                sscanf(argv[2],"%f",&gain);
//              printf("gain = %f\n",gain);
                if((out = fopen(argv[3],"wt")) == NULL)
                {
                        printf("Error opening output file");
                        exit(0);
                }
                fprintf(out,"%d\n",DATAPOINTS);
                fprintf(out,"%f\n",gain);
                current_value = (int) current;
                fprintf(out,"%d\n",current_value);
                fprintf(out,"%d\n",MEASUREMENTS);
                fprintf(out,"%d\n",FASTMEASUREMENTS);
                fprintf(out,"%d\n",FASTDATAPOINTS);
                fprintf(out,"%f\n",meas_time);
        }

// Initial Impedance measurement

        measure(argc,dc,data,current_value,out);
        avg=0;
        for(m=DATAPOINTS-100;m<DATAPOINTS;m++)
                avg = avg + data[m];
        avg = (avg / 10);
        r1 = 1000*(.006*avg-.005)*255 / (current*2.89*gain);
        printf("r1 = %f\n",r1);

// Initialize Oscilloscope
```

```
        initialize();
        hpsend(":WAV:FORM BYTE\n",10);
        hpsend(":WAV:SOUR CHAN1\n",10);
        hpsend(":WAV:POIN 500\n",10);
        printf("Scope Setup Completed\n");

//      Impedance measurements and pulsing

        pulse();
        time(&time_zero);
        printf("Pulse finished\n");
        outportb(PRINTER_CONTROL_PORT,WRITE_MODE);
//      outportb(PRINTER_DATA_PORT,0);

        printf("End of pulse detected\n\n");
        fastmeasure(argc,fdata,current_value,out);
        printf("Fast measurements completed\n");

//      Delay until measurement at 1 second
        for(i=1;i<275;i++)
                time(&time1);
        measure(argc,dc,data,current_value,out);
        avg=0;
        for(m=DATAPOINTS-100;m<DATAPOINTS;m++)
                avg = avg + data[m];
        avg = (avg / 10);
        r2 = 1000*(.006*avg-.005)*255 / (current*2.89*gain);
        printf("r2 = %f\n",r2);
        avg = r2/r1;
        printf("r2/r1 = %f\n",avg);

        printf("Impedance Measurements Finished\n Downloading data from scope\n");

        if (argc == 4)
        {

// Get data during pulse from osciloscope
        hpsend(":WAV:DATA?\n",1);
        hpget(answer,511);

// Write data to file if a filename was given

                for (j=1;j<512;j++)
                {
//                      printf("%d, pulse data = %d\n",j,answer[j]);
                        fprintf(out,"%d\n",answer[j]);
```

```
                }

        hpsend(":WAV:SOUR CHAN2\n",10);
        hpsend(":WAV:DATA?\n",1);
        hpget(answer,511);

// Write data to file if a filename was given

                for (j=1;j<512;j++)
                {
//                      printf("%d, pulse data = %d\n",j,answer[j]);
                        fprintf(out,"%d\n",answer[j]);
                }
        }
        fclose(out);
}
```

B2 Matlab code for data analysis

B2.2.1 datafit.m

```
function [foutf,respf,fitoutf,out,resp,fitout] = datafit(filename)

% [out,resp,fitout] = datafit(filename)
% This function takes as its argument a data file produced by the
% the PC-based data acquisition system. It takes the Fourier transform
% of each measurment and calculates the cicuit element values R1, R2,
% C1 and C2. The output is in the form of six matrices, with each row
% representing the results of a measurement at adifferent time point. The
% matricies are divided into two groups of three. The first three contain
% the information from the 2 msec measurements made up to 540 msec
% post pulsing, and the second three matricies contain the information
% from the measurements starting at one second after the pulse.
% In each group of three matricies, the first contains the values of the
% circuit elements R!, R2, C1, C2, the second contains the measured
% frequency response, and the third contains the curve resulting from
% the least squares best fit to the cicuit model.

% define constants
sampfreq = 10000;
[len,foo] = size(filename);

% Extract information from file header
header_size = 7;
datapts = filename(1);
gain = filename(2);
gain = 47/(10-gain);
current1 = filename(3);
current2 = filename(4);
timepts = filename(5);
fastdatapts = filename(7)
fastmeasurements = filename(6)

% Calculate additional constants
times = zeros(1,timepts+1);
times(1) = 0;
times(2:timepts+1) = filename(1+header_size:header_size+timepts);
time = linspace(0,fastdatapts,fastdatapts) ./ sampfreq;

% Process fast measurements

current = current2;

% Calculate times of each fast measurement
for i=1:fastmeasurements,
        ftimes(i) = 27 + (i-1)*6;
end
```

```
% Step through each fast measurement and analyze
for i=2:fastmeasurements,

        offset = header_size+timepts+datapts+(i-1)*fastdatapts;
        data = filename(offset+1:offset+fastdatapts);

        [fout(i-1,:),fresp(i-1,:),foutf(i-1,:)] = dofit(data,current,gain);
end

% Calculate data offset for measurement starting at one second
base = header_size+timepts+datapts+fastmeasurements*fastdatapts;
total_data = filename(base:len);

% Calculate constants
time = linspace(0,datapts,datapts) ./ sampfreq;

% Loop for each measurement
for i = 1:timepts,

        if i==1
                % Get pre-pulsing measurement
                offset= header_size+timepts;
                % Use pre-pulsing current
                current = current1;
        else
                % Get post pulsing measurements
                offset = base+(i-1)*datapts;
                % Use post-pulsing current
                current = current2;
        end

        %Extract data for measurement i
        data = filename(offset+1:offset+datapts);
        [out(i,:),resp(i,:),fitout(i,:)] = dofit(data,current,gain);
end
resp(:,i+1) = f;
fitout(:,i+1) = ffit;
hold off;
```

B2.2 dofit.m

```
function [K,p] = labfit1z1p(no_sings)

% Fits Data to specified number of poles and zeros
%
% Calls f1z20.m (error function for least squares fitting routine
%
% Remeber, Data must be Global...

global Data
```

```
%OPTIONS=0;
OPTIONS(5)=1;
OPTIONS(7)=1;
OPTIONS(2)=1e-2;

pz = zeros(1,3);

% Initial guesses
        pz(1) = 150;
        pz(2) = 90;
        pz(3) = 1000;

% call least square fitting routine, with error function
[p,OPTIONS]=leastsq('f1z2p',pz);

%
f = Data(:,1); y = Data(:,2);
s = j*2*pi*f;

% Calculate return values
A = abs((s + p(1))./((s+p(2)) .* (s + p(3))));
K = A\y;
```

B2.3 labfit1z2p.m

```
function [out,resp,fitout]=dofit(data,current,gain)

%
% [out,resp,fitout]=dofit(data)
% Takes Fourier transform of data, fits the data to a 1 zero and 2 pole
% model, returns element values (R1,R2,C1,C2), frequency response and
% the best fit curve to the frequency response.
%
% Calls labfit1z2p.m
%

        % Translate data into actual impedance values
        data = 1e6*(.006*data - .005)*255 ./ (current*2.89*gain);

        % Take fft of derivative of step response
        deriv = zeros(datapts,1);
        for n=1:datapts-1,
                deriv(n) = (data(n+1)-data(n))*sampfreq;
        end
        deriv(datapts) = deriv(datapts - 1);
        fft_data= abs(fft(deriv))/sampfreq;
        disp('Done taking derivative')

        %
        subplot(223)
        plot(time,data,'m');
        figure(gcf)
```

```
        % Remove DC component due to saline

        fft_data = fft_data - 250;

        % Create corresponding frequency vector

        N = length(fft_data);
        freq = ones(N,1);
        for n=1:N,
                freq(n) = sampfreq * (n-1) / N;
                if freq(n) <200,
                        m=n;
                end
                if freq(n) < 500,
                        l = n;
                end
                if freq(n) < 56.0,
                        window_low = n;
                elseif freq(n) < 64,
                        window_high = n;
                end
        end

        if (window_high-window_low == 1),
                window_high = window_low+2;
        end

% Eliminate data points near 60 Hz and truncate frequency response

        f = [freq(1:window_low) ; freq(window_high:m)];
        data = [fft_data(1:window_low) ;fft_data(window_high:m)];
        fplot = [freq(1:window_low) ; freq(window_high:l)];
        dataplot = [fft_data(1:window_low) ;fft_data(window_high:l)];

        % Least Squares Fitting for impedance measurements

        global Data
        Data = [f data];
        figure(gcf)
        ffit = [1; 2; 4; 8; 10; fplot];
        %ffit=fplot;
        s = j*2*pi*ffit;
        % Fit to 1 zero two pole model
        [K,pz] = labfit1z2p(3);
        %fit = f1z2p(pz);
        %mse = sum(fit .* fit) / length(fit);
        fitcurve = K*abs((s + pz(1)) ./ ((s + pz(2)) .* (s + pz(3))));
        z = pz(1);
        p1 = pz(2);
        p2 = pz(3);

        % Element Values for old model
        C1 = 1/K;
```

```
        R1 = K*pz(1)/(pz(2)*pz(3))
        R2 = K / (pz(2) + pz(3) - pz(1) - (pz(2)*pz(3)/pz(1)));
        C2 = 1/(R2*pz(1));

        % Calculate ouput matricies
        out = [times(i) R1 R2 C1 C2 DC];
        resp = data;
        fitout = fitcurve;
        % Plot data and fit

        subplot(224)
        semilogx(fplot,dataplot,'co',ffit,fitcurve,'m')
        hold on;
        grid on;
        figure(gcf)
end
```

B2.4. f1z2p.m

```
function fit = f1z2p(pz)

%
%       fit=f1z2p(pz)
%       Error function passed to leastsq.m routine. Computes error
%       between the data and the values computed by the current
%       function of 2 poles and 1 zero. pz is of the form:
%
%       [zero pole]
%
%       Also computed is K, the multiplicative gain factor.

global Data

% Global Data
f = Data(:,1); y = Data(:,2);
s = j*2*pi*f;

% Calculate the current impedance function
A = abs((s + pz(1)) ./ ((s+pz(2)) .* (s + pz(3))));
K = A\y;
z = A*K;

% Compute error (calculated impedance - data)
fit = z-y;
```